agso RESEARCH NEWSLETTER

'Geoscience for Australia's Future'

Number 26 May 1997

Mineral-mapping in the north Pilbara Craton

A directed-principal-components-of-band-ratios method for correlating Landsat-5 Thematic Mapper spectral data with geology

Andrew Y. Glikson[1]

The application of multispectral image data to 1:100 000 mapping programs for the National Geoscience Mapping Accord

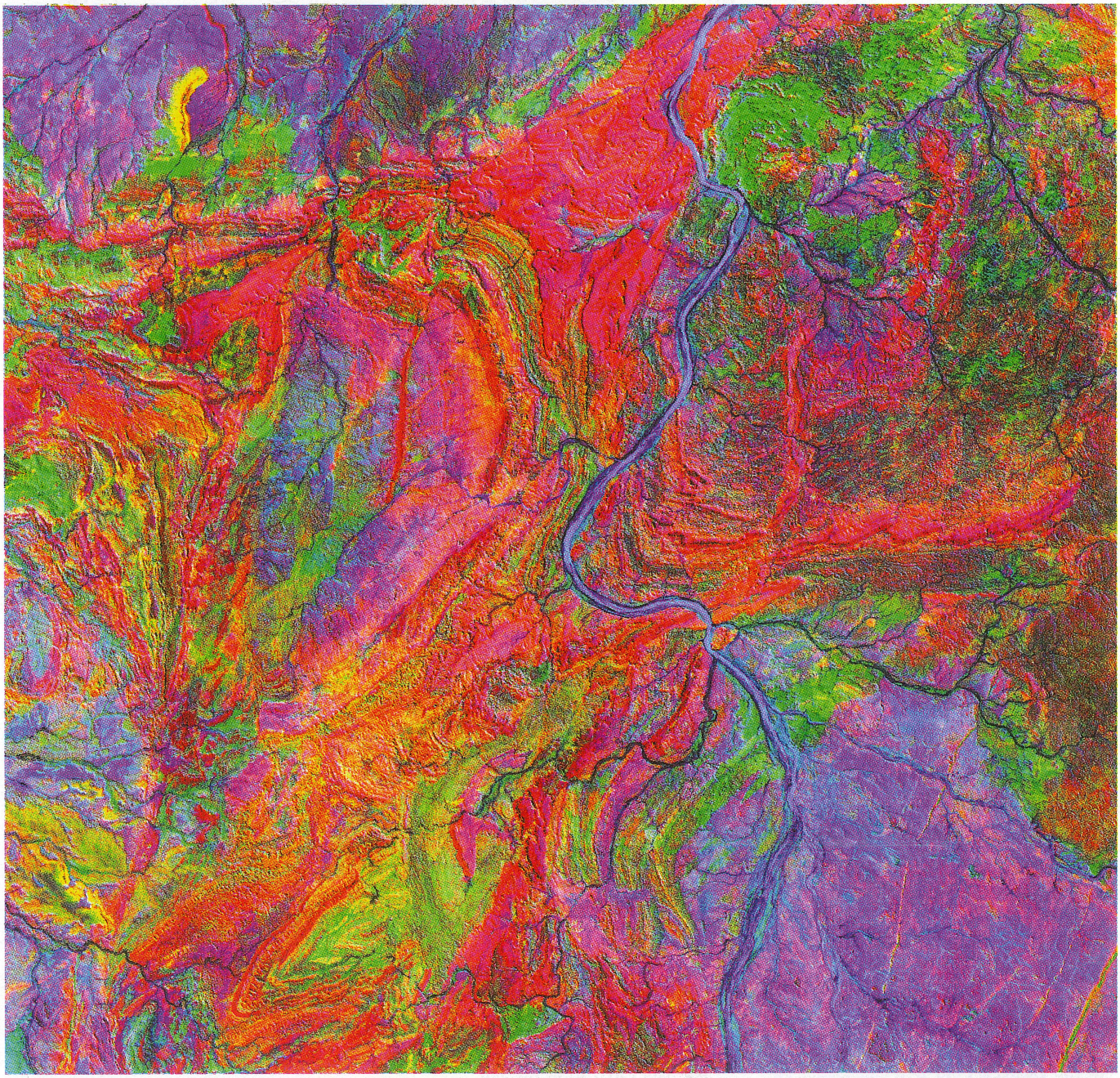

Fig. 1. A directed-principal-components RGB pc2(4/3; 5/7):5/4:1+7 image of most of the North Shaw 1:100 000 Sheet area, north Pilbara Craton, Western Australia. The Strelley Granite appears as a blue elliptical body with a red collar at centre left.

Table of Contents on page 2

AGSO

Australian Geological Survey Organisation

A research organisation of the Department of Primary Industries & Energy

AGSO JUBILEE 1946-96

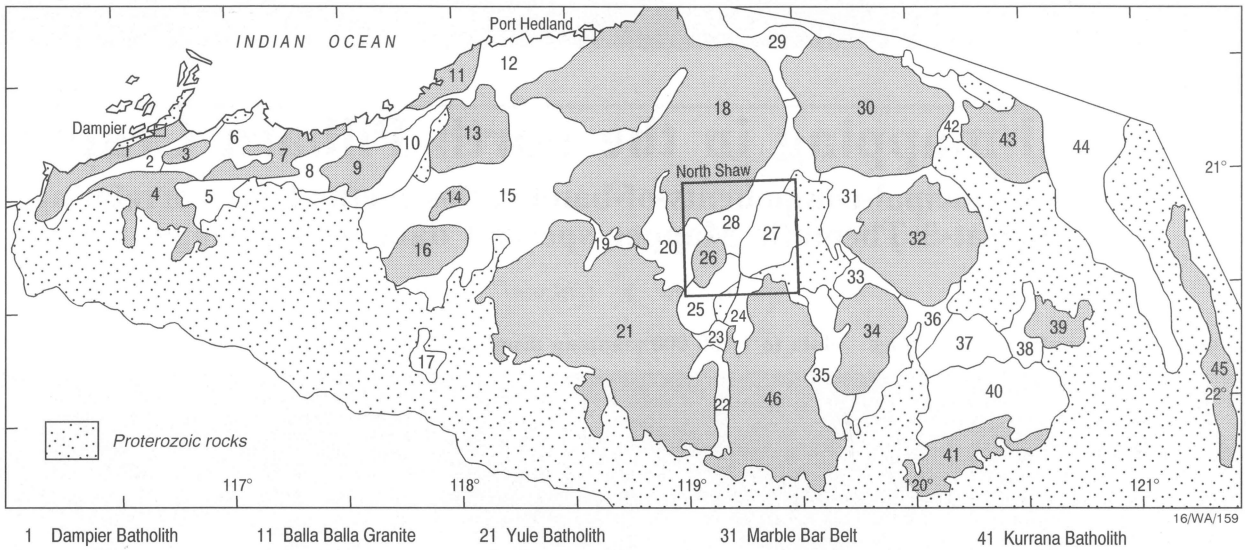

1 Dampier Batholith
2 Regal Belt
3 Karratha Granite
4 Chiratta Batholith
5 Sholl Belt
6 Roebourne Syncline
7 Harding Granite
8 Sherlock Belt
9 Caines Well Granite
10 Whim Creek Belt
11 Balla Balla Granite
12 Boodarie Belt
13 Portree Granite
14 Peawah Granodiorite
15 Mallina Synclinorium
16 Satirist Granite
17 Nunyerry Inlier
18 Carlindi Batholith
19 Wodgina Belt
20 Pilgangoora Syncline
21 Yule Batholith
22 Western Shaw Belt
23 Tambina Complex
24 North Shaw Belt
25 Soanesville Belt
26 Strelley Granite
27 North Pole Dome
28 Lalla Rookh Syncline
29 Goldsworthy Syncline
30 Muccan Batholith
31 Marble Bar Belt
32 Mount Edgar Batholith
33 Warrawoona Syncline
34 Corunna Downs Batholith
35 Coongan Syncline
36 Kelly Belt
37 McPhee Dome
38 Mount Elsie Belt
39 Yilgalong Granite
40 Mosquito Creek Synclinorium
41 Kurrana Batholith
42 Shay Gap Syncline
43 Warrawagine Batholith
44 Canning Basin
45 Gregory Granitic Complex
46 Shaw Batholith

Fig. 2. Geological sketch map of the north Pilbara Craton, Western Australia, showing principal greenstone belts, granitic batholiths, and outliers of the late Archaean to early Proterozoic Hamersley Basin (stippled).

(NGMA) depends critically on the identification of consistent lithological correlations. Landsat-5 Thematic Mapper (TM) multispectral data in the visible, near-infra-red, and short-wave infra-red ranges, enhanced by advanced image-processing analysis and tested in the field, provide a powerful tool for the interpolation and extrapolation of geological and environmental attributes in the context of the geological mapping. The good exposure under the arid conditions of the north Pilbara region, combined with the good expression of primary lithological variations by their distinct weathering products, facilitates effective correlations between multispectral sensor data and original rock types. A directed-principal-components-of-band-ratios method tested in this region evinces consistent relationships between the enhanced image data and minerals such as clays, iron oxides, and quartz in weathering crusts. This correlation has applications for both lithological and mineral-alteration mapping.

In the north Pilbara Craton (WA), an Archaean (3.5–2.7 Ga) greenstone–gneiss–granite terrain is overlain by outliers of the ca 2.7-Ga Fortescue Group of the Mount Bruce Supergroup (Fig. 2; Hickman 1983: Geological Survey of Western Australia [GSWA], Bulletin 127). Part of a systematic NGMA 1:100 000-scale mapping program of this terrain by GSWA and AGSO is directed towards a study of:

- Landsat–5-TM multispectral (7-band) visible to short-wave infra-red satellite scanner data (30 × 30 m pixels);
- Spot panchromatic image data (10 × 10 m pixels); and
- Geoscan Mark-I airborne multispectral (13-band) image data (10 × 10 m pixels).

The geographical coverage of the various types of image data is indicated in Figure 3. This article reports on progress in Landsat–5-TM spectral–lithological correlations in the Pilbara during 1995–96, and coincides with the release of digital and hard copy Landsat–5-TM image products*.

Objectives

The principal objectives of the north Pilbara multispectral remote-sensing study include:

- discriminating between tholeiitic basalts and komatiites;
- identifying felsic volcanic and sedimentary rocks;
- differentiating between extrusive and intrusive ultramafic units;
- identifying alteration zones;
- differentiating between granitoid phases in batholiths;
- tracing faults, shear zones, and dykes; and
- identifying the compositions and thereby the sources of alluvial and creek bed deposits, including the locations of lateritic zones and calcrete deposits.

Tests of the attributes of a range of alternative image-processing methods showed that a directed-principal-components-of-band-ratios method producing RGB (red, green, blue) pc2 [4/3;5/7]:5/4:1+7 images is particularly suitable for correlating a wide range of surface

* The imagery covers seven-and-one-half Landsat–5-TM (185 × 185 km) scenes over a total area of ca 140 000 km^2, and includes algorithms for forty-six 1:100 000 Sheet areas covering a total area of ca 115 000 km^2 broadly defined by latitudes 20°00′–22°00′S and longitudes 116°00′–121°00′E. Scenes include the Dampier, Yarraloola, Roebourne, Pyramid, Port Hedland, Marble Bar, Nullagine, and southern Yarrie 1:250 000 Sheet areas. For more information, see *AUS.GEO News 40*, for June 1997, or contact Richard Blewett, Pilbara Project Leader, at AGSO (tel. +61 6 249 9713 or e-mail rblewett@agso.gov.au).

In this issue:

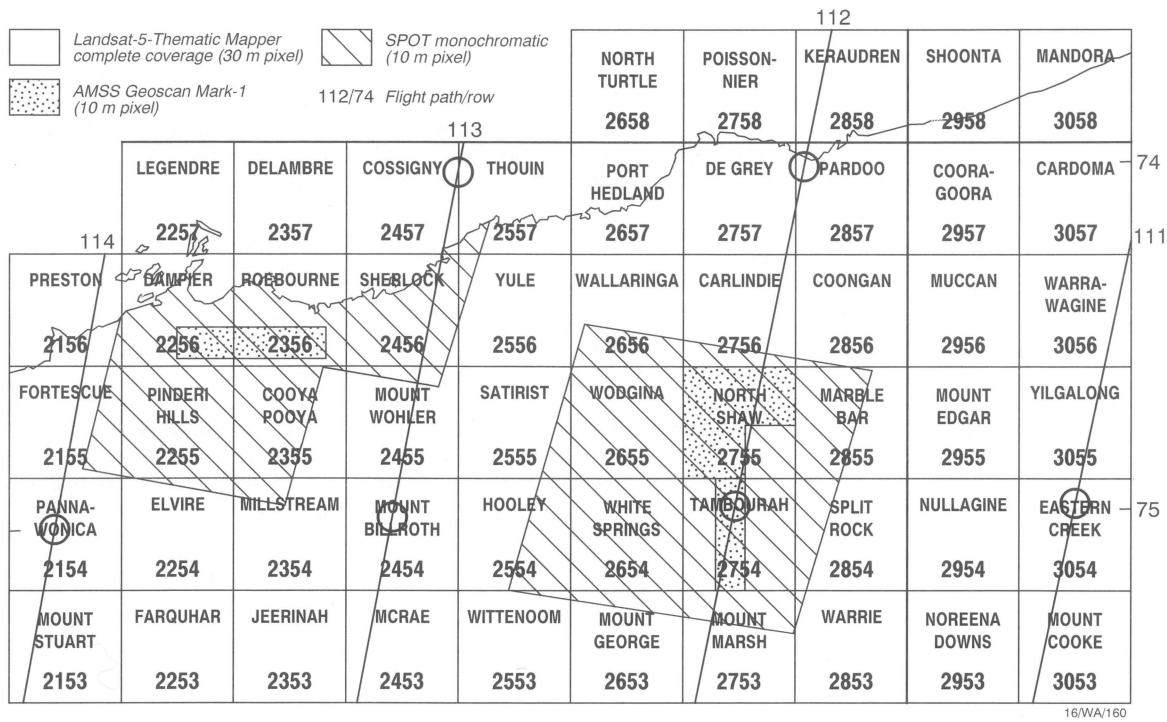

Fig. 3. Distribution of Landsat–5-TM scenes, panchromatic Spot imagery, and Airborne Multispectral Scanner Geoscan Mark–I data runs applied by AGSO in the Pilbara region.

material types and morphological–drainage features under the arid conditions of inland Australia (Glikson & Creasey 1995: AGSO Journal of Australian Geology & Geophysics, 16 (1 & 2), 173–193). Field tests of this method in the Pilbara were conducted during 1995–96. They were assisted by an extensive geochemistry database developed by AGSO and GSWA during previous investigations (Glikson & Hickman 1981: BMR Record 1981/36; Glikson et al. 1986: BMR Record 1986/6; Glikson et al. 1987: BMR Record 1987/30). The geochemical data aid correlations between the image data and the compositions of the rocks in the areas sampled.

Methodology

False-colour composites of Landsat–5-TM images reflect the main constituents of natural weathering surfaces. Thus, an RGB–741 combination generally shows iron oxides in red; green vegetation as green; and clays as blue; however, the effects of scene brightness variations dominate the raw bands, and mask spectrally significant information, which may be lost in shadowed areas. Band ratios eliminate the multiplicative effects, but spectral superposition of vegetation and clay — particularly in the 5/7 ratio — make interpretation difficult. However, the loss of the albedo brightness–shadow effect in band-ratio images renders it difficult to determine locations and thus to use them in the field. The application of directed-principal-components analysis to the 4/3 and 5/7 band ratios favours better discrimination of clays (Fraser & Green 1987: International Journal of Remote Sensing, 8, 525–532).

In the Pilbara study, the following choices of RGB components promoted maximum discrimination between weathering materials, and reflected the morphological features of the terrain.

Red channel — pc2(4/3;5/7). Drainage arteries throughout the region are characterised by abundant eucalypts and low clay contents. If the high 4/3 signature of the eucalypts is suppressed, these features display low reflectance values which provide excellent morphological control in the directed pc2(4/3;5/7) imagery. This control reflects:

- the high correlation of 4/3 and 5/7 band ratios shown by green vegetation;
- the low correlation of these band ratios for clay; and
- the selection of the second principal component (i.e., of clay) effected by the principal-components method.

Consequently, the drainage system is marked by dark to black outlines. This is shown in an RGB pc2(4/3;5/7):5/4:1+7 image of the North Shaw 1:100 000 Sheet area (Fig. 1).

Green channel — 5/4 band ratio: Iron oxide components are generally discriminated by the high 3/2 band ratios of hematite and goethite — components difficult to discriminate from one another in Landsat–5-TM imagery. However, dry vegetation has a similarly high 3/2 band ratio, which obscures the iron oxide signature. Hematite — the normally dominant iron oxide in the Pilbara — displays a uniquely high 5/4 band ratio, which was selected to represent iron oxides in the Pilbara study.

Blue channel — bands (1+7): Materials yielding the highest reflectance in all bands include quartz and silcrete. In particular, coarse quartz in granitoid rocks, and abraded clastic quartz in mature arenite and in alluvial sands in creek beds, reflect strongly in all bands, as confirmed by field correlations. The sum of reflectance values of bands 1 and 7 can be used in this regard. By contrast, use of only the lower or higher band will favour clay or iron oxide respectively.

Outcrops throughout the Pilbara craton are variously covered by dry spinifex and grass and — in the more humid areas, particularly near the coast — also by lichen. Where the vegetation is dense, it may partly mask the rocks with the 5/7 band-ratio signature of dry vegetation and to a lesser extent the 4/3 signature of green chlorophyll-rich vegetation. However, the semi-aridity of the Pilbara favours the exposure of a high proportion of rock-weathering surfaces, facilitating spectral–lithological correlations. As a result, unique lithological signatures are evident in Landsat–5-TM spectra, including:

- the characterisation of iron oxides of laterites and weathered magnetite-rich gabbro, dolerite, and pyroxenite by high 5/4 band ratios, distinct from the spectral signature of spinifex and lichen, and
- the expression of quartz-rich rock types such as granitoids, whose strong reflectance is normally masked by a vegetation signature only to a minor extent.

According to the foregoing discussion, RGB pc2(4/3; 5/7):5/4:1+7 images facilitate the expression of four factors: clay, iron oxide, quartz, and drainage patterns. Advantages of this method include:

- the discrimination of visually sensitive red–green (clay–iron oxide) mixtures, which — along with silica and carbonate — dominate weathering crusts in the Pilbara region;
- the good expression of drainage systems; and
- the consequent direct lithological and morphological information allowed by these images.

Spectral–lithological correlations

Spectral–lithological interpolation and extrapolation of field data can be applied as a mapping tool in an area only after correlations have been established by rigorous testing — primarily from detailed ground observations identifying surface processes and structural and textural characteristics. Ideally, field spectrometers, or X-ray and thin-section studies of weathering crusts and their parental materials, also should be used to test the correlations.

The following correlations of RGB pc2(4/3;5/7):5/4:1+7 images are based solely on field and microscopic observations:

- *peridotite* — Mg-hydrosilicate (chlorite, serpentine)-rich weathering crusts appear crimson red, or shades of purple where they are accompanied by vein quartz detritus (blue);
- *pyroxenite* — phyllosilicate- and iron oxide-dominated weathering crusts appear green;
- *gabbro* — iron oxide- and clay-dominated weathering crusts appear green to light red;
- *high-Mg to peridotitic komatiitic volcanics* — phyllosilicate-dominated weathering crusts appear deep crimson red;
- *mafic volcanics* — iron oxide-dominated (+ clay-mix) weathering crusts appear light green with yellow and reddish tinges;
- *doleritic dykes* — marked iron oxide-rich weathering crusts appear green;
- *felsic volcanics* — clay- to iron oxide-dominated weathering crusts appear mottled red to yellow tinged with green; structurally controlled drainage patterns;
- *feldspathic sandstone* — similar to felsic volcanic signatures, but show dendritic drainage patterns;
- *granitoids* — dominated by quartz and clay-rich arkosic weathering products, which appear blue to purple; blue is particularly marked in fire-burnt areas; where both blue and red are suppressed by thick vegetation, a compensatory green is shown;
- *banded iron formations* — surprisingly display dominant clay signatures mixed with iron oxide, owing to the universal interbanding of these rocks with siltstone units, and the abundance of flat-lying silt-coated slabs around outcrops;
- *lateritic deposits* — commonly occur as relict plateau and flat hill tops (mesa) appearing deep apple green;
- *alluvial mafic source-derived detritus and creek deposits* — iron oxide and clay signatures appear yellow to green;
- *alluvial quartz-rich felsic source-derived detritus and creek bed sand* — markedly represented in the blue; major creeks display strongly in the blue, and form corridors fringed by black, which represents the removal of the green vegetation signature of fringing eucalypts.

Some problems remain — for example, the commonly strong but unexplained 5/7 band-ratio signatures that are associated with vein quartz and chert units, and may represent thin clay coatings. Further field and laboratory spectrometric measurements should allow fine tuning of satellite and airborne multispectral correlations as one of the essential prerequisites for the next generation of geoscientific maps.

Applications

Geological mapping during 1995–96 has contributed to the identification of phyllosilicate (clay) alteration patterns within mafic volcanic rocks, displayed as high 5/7 band-ratio anomalies within host basalts of high 5/4 band ratio. Examples occur in mafic volcanics of the Gorge Creek Group which underlie volcanogenic massive sulphides flanking the Strelley Granite (Fig. 1). The phyllosilicate alteration is associated with pods of sulphide, facilitating field and remote scanner-based economically oriented alteration mapping.

Used in conjunction with geological maps of the same scale, the enhanced Landsat–5-TM-image 1:100 000 data sets will enable users to make detailed comparisons between stratigraphic interpretations and lithological indicators. Such comparisons should help to focus further field observations on details too fine for cartographic presentation. It should be borne in mind that, although the multispectral scanner data invariably represent mineralogically and chemically significant information, they do not always facilitate a geological interpretation, but are more likely to where they are supported by field spectrometry and/or X-ray analysis. A combination of airborne (small-pixel) multispectral surveys and field spectrometry is seen as the next step toward further refinement of spectral–lithological correlations.

[1] c/o Dr R. Blewett, Minerals Division, Australian Geological Survey Organisation, GPO Box 378, Canberra, ACT 2601; tel. +61 6 288 1732, fax +61 6 288 1792, e-mail aygsearch@cos.com.au.

Proterozoic thrusting in the Osmand Range area of the East Kimberley, Western Australia

David H. Blake[1]

Structural repetitions of northerly dipping Palaeoproterozoic rocks identified in the Osmand Range area (Turkey Creek 1:100 000 Sheet area; Figs. 4–6.), East Kimberley, are attributed to thrusting possibly related to the Yampi Orogeny, a major Mesoproterozoic deformation event in the West Kimberley. The thrusts displace metasediments and plutonic rocks of the basement and unconformably overlying sedimentary rocks and basaltic volcanics that I assign to the Kimberley Group.

The basement metasediments can be considered prospective for gold, as they are probably correlatives of lithologically similar turbiditic and calcareous rocks in the 1880–1840-Ma Halls Creek Group, the host for lode gold deposits near Halls Creek to the south. However, no alkaline volcanics like those spatially associated with many of the Halls Creek gold deposits (Hoatson et al. 1995: AGSO Research Newsletter 22, 1–2) are known in the Osmand Range area. The metasediments were deformed and metamorphosed before being intruded in the northern part of the area by the McHale Granodiorite (1827 ± 3 Ma*) and by gabbro. The overlying Kimberley Group, which was probably laid down at around 1800 Ma, is intruded by Hart Dolerite sills (1790 Ma*) in the Kimberley Basin (to the west). In the Osmand Range area, it is overlain unconformably by the Mount Parker Sandstone and Bungle Bungle Dolomite, which are considered to postdate the thrusting and also local folding of the Kimberley Group. According to Kath Grey (GSWA, personal communication 1997), stromatolites in the Bungle Bungle Dolomite indicate a probable late Mesoproterozoic (1200–1000 Ma) age.

The thrusts described below are not shown as such on the latest geological map (Tyler et al. 1997: 'Turkey Creek, W.A., Sheet 4563'; Geological Survey of Western Australia, 1:100 000 Geological Series), on which the rocks that I have mapped as the Kimberley Group (Figs. 5 and 6) are shown instead as the Red Rock Formation and Texas Downs Formation.

The Osmand Range area (Fig. 4) lies to the east of the north-northeasterly trending Halls Creek Fault Zone, a major strike-slip structure which to the north displaces rocks as young as Devonian. In this area two subparallel major ridges trending east-northeast are separated by a general depression in which there are many smaller and lower ridges. The southern major ridge is the Osmand Range, and the depression to the north is the valley of the easterly flowing Osmand Creek. Both major ridges are formed mainly of northerly dipping Kimberley Group overlain by the Mount Parker Sandstone and Bungle Bungle Dolomite. Basement rocks are exposed in the depression between the two ridges and to the south of the Osmond Range. A large splay from the Halls Creek Fault Zone to the west, the east-northeasterly trending Osmand Fault, separates the northerly

* Dated by R.W. Page; AGSO's OZCHRON database.

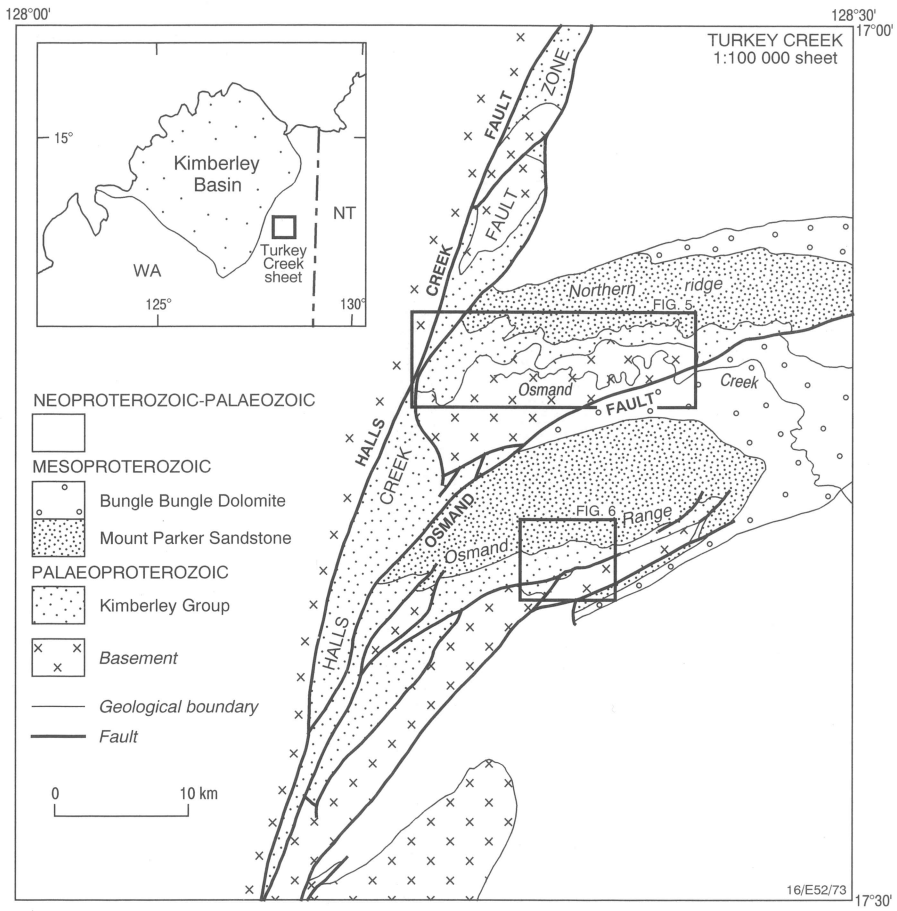

Fig. 4. Locality map.

dipping sequence forming the Osmand Range from the basement rocks of the Osmand Creek valley.

According to my interpretation, the Kimberley Group in the Osmand Range area is represented by two formations of ridge-forming clean quartz sandstone (both previously mapped as the Red Rock beds) and an intervening stratigraphic marker unit of recessive amygdaloidal basalt lava flows (previously mapped as the Fish Hole Dolerite). Variations in thickness of the lower sandstone formation, which I assign to the King Leopold Sandstone, are partly a result of deposition on an irregular surface. Fluvial red-bed-type sandstone, 0–100 m thick, is locally present at the base, but most of this formation consists of up to 300 m of coarse-grained quartz sandstone, the lower part of which commonly contains angular to subangular clasts up to cobble-size of quartzite, vein quartz, and jasper. The King Leopold Sandstone has a characteristic rough texture on airphotos. In contrast, the upper sandstone formation, the Warton Sandstone, is generally finer-grained and better sorted, and on airphotos has a smoother texture and shows well-defined, closely spaced bedding lines. The intervening unit of basaltic lavas, the Carson Volcanics, commonly includes some thin bands of sandstone ranging from quartz-rich to highly lithic. The two youngest formations of the Kimberley Group in the Kimberley Basin — the Elgee Siltstone and overlying Pentecost Sandstone — are not present in the Osmand Range area, but can be identified a short distance to the west, overlying the Warton Sandstone in fault blocks within the Halls Creek Fault Zone. Hence all formations of the Kimberley Group, as described and defined by Gellatly et al. (1975: BMR Report 152), can be recognised east of the Halls Creek Fault Zone in the Turkey Creek 1:100 000 Sheet area. This implies that the Kimberley Basin once extended well to the east of the Halls Creek Fault Zone.

Thrusts have been recognised along the southern sides of both major ridges in the Osmand Range area. The southern side of the northern ridge is an irregularly stepped scarp capped by the Mount Parker Sandstone; each step is a ledge of northerly dipping Kimberley Group sandstone partly bounded by faults. Evidence for thrusting along this scarp includes exposures in sandstone cliffs of low-angle faults dipping north at slightly steeper angles than bedding, a narrow strip of basement rocks underlain and overlain by Kimberley Group sandstone (along section line C–D, Fig. 5), and repetitions of the King Leopold Sandstone and Carson Volcanics up the scarp. Local excessive thicknesses of the King Leopold Sandstone and Carson Volcanics here may be results of thrust repetitions. In places, the positions of thrusts are marked by brecciated sandstone and by narrow bands of mafic phyllonite representing highly sheared basalt. The thrusts are offset along strike by numerous cross-cutting younger faults. The thrusts shown in Figure 5 repeat part of the King Leopold Sandstone along section line A–B, parts of the basement and King Leopold Sandstone along section line C–D, and parts of the King Leopold Sandstone and Carson Volcanics along section lines E–F and G–H. The abnormally large thickness (about 500 m) of the Carson Volcanics along the northern part of section line G–H may be an example of repetition by an unmapped thrust or thrusts.

To the south, along the south side of the Osmand Range, several thrusts are photo-interpreted within the Warton Sandstone where this formation, dipping generally northwards at 25–55°, is abnormally thick (more than 1 km). A major fault separates the Warton Sandstone from the King Leopold Sandstone and basement metasediments farther south, and to the north the formation is overlain unconformably by less steeply dipping Mount Parker Sandstone (Fig. 6). The Warton Sandstone here has the typical airphoto pattern of smooth texture and closely spaced bedding lines, but it also shows several narrow recessive bands which are slightly oblique to bedding. These narrow bands are interpreted as northerly dipping thrusts which repeat parts of the Warton Sandstone. Both bedding and interpreted thrusts in the Warton Sandstone were tightly folded before the deposition of the overlying Mount Parker Sandstone and Bungle Bungle Dolomite. The thrusting here, like that on the northern ridge, indicates movement from north to south.

The foregoing observations have led to the following conclusions:

- the Kimberley Group, and hence also the Kimberley Basin in which it was laid down, extended well to the east of the Halls Creek Fault; and
- the Kimberley Group and underlying basement rocks in the Osmand Range area were thrusted and folded before the Mesoproterozoic Mount Parker Sandstone was deposited. This deformation may be related to the Yampi Orogeny in the West Kimberley, which probably took place after 1300 Ma but before 1000 Ma (Griffin et al. 1993: 'Lennard River, Western Australia, 1:250 000 Geological Series'; Geological Survey of Western Australia, Explanatory Notes, SE/58–8, 3rd Edition). It is much older than the thrusting in the Albert Edward Range, to the south, which involved the Neoproterozoic Albert Edward Group and Lower Cambrian Antrim Plateau Volcanics.

[1] Minerals Division, Australian Geological Survey Organisation, GPO Box 378, Canberra, ACT 2601; tel. +61 6 249 9667, fax +61 6 249 9983, e-mail dblake@agso.gov.au.

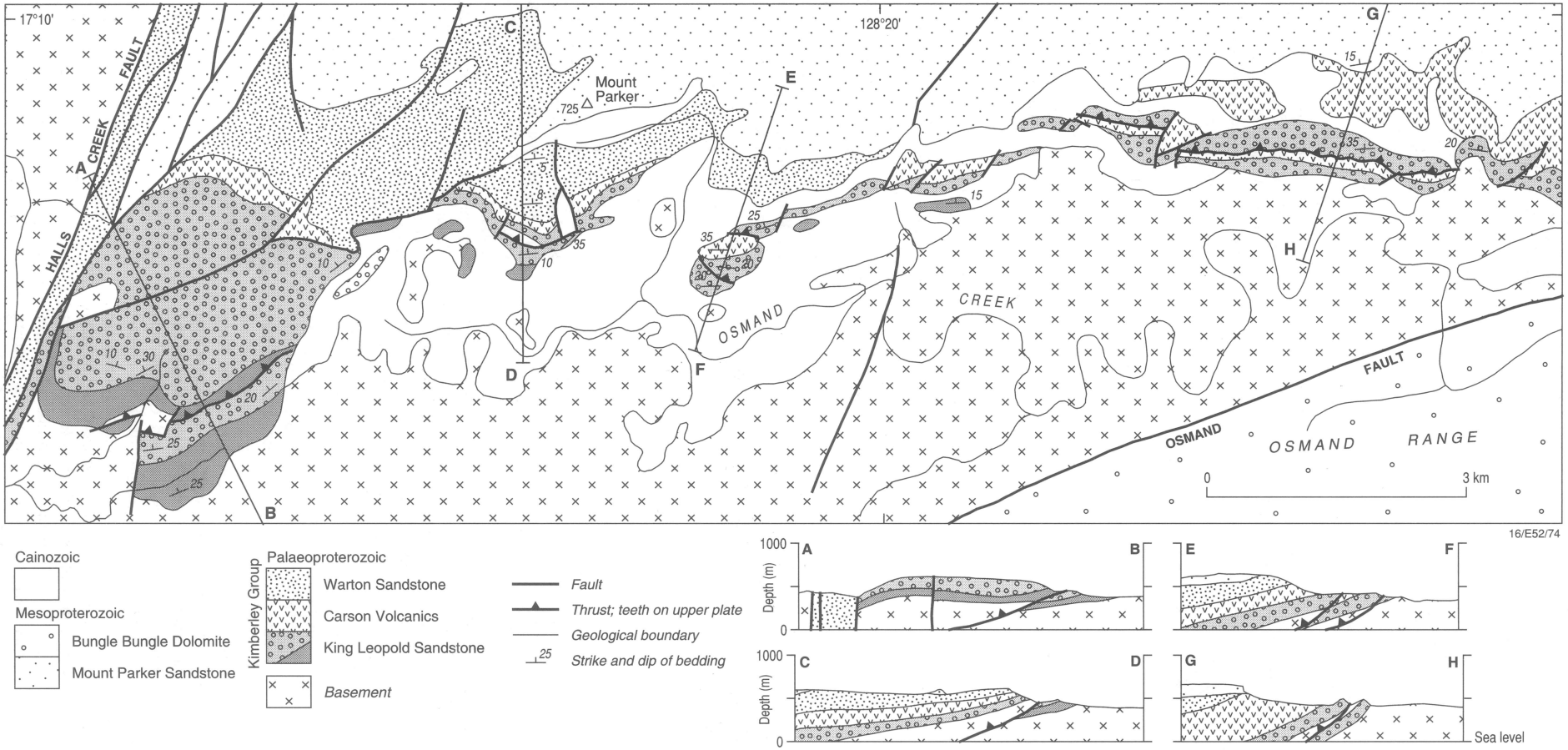

Fig. 5. Thrusts along the southern side of the northern ridge, Osmand Range area.

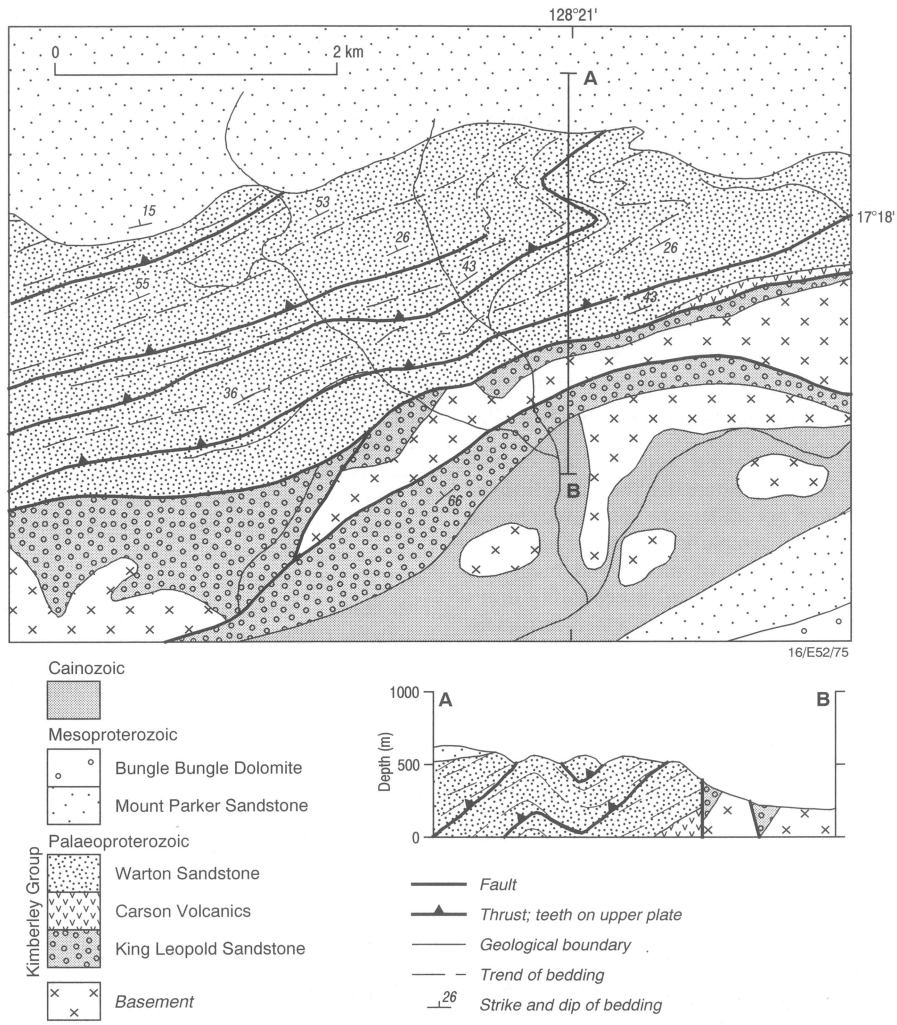

Fig. 6. Folded thrusts in the Warton Sandstone, Kimberley Group, on the south side of the Osmand Range.

Rock magnetism gets under way in AGSO

John Giddings[1] & Chris Klootwijk[1]

With the recent purchase and installation of perhaps the world's most sensitive, commercially available instrument for measuring the magnetic susceptibility of rocks — the Czech-made KLY3S spinner kappabridge and CS3 furnace unit — AGSO has catapulted its capability to measure magnetic susceptibility from a rudimentary level to that of a competitive leader. Consequently, AGSO is ensuring that, in the data it supplies and in the studies it conducts, it maintains an advantage. We examine the need for this instrument and illustrate the types of information it can supply.

The magnetism of rocks

The magnetism of rocks is perhaps the oldest geophysical property employed as a tool by man: it was used for navigation in early historical times. Nowadays, it provides geoscientists with one of the most versatile tools they have for studying and understanding geological processes. Its versatility stems from the fact that it is the only geophysical property that can also be evaluated over geological time. We can use it to date and correlate rock units; date folding, faulting, and uplift; date and map fluid movement and chemical alteration; date the magnetic by-products of mineralisation; map surface and subsurface geological boundaries; reconstruct ancient continental configurations and movements; determine palaeolatitudes; use it as a proxy for environmental change and as a tracer in provenance studies; and determine magnetic fabrics for use in magnetic anomaly modelling, and as indicators of ancient stress-fields, flow, and palaeocurrent directions.

The source of these diverse applications, however, is just a few magnetic minerals: those minerals which, at ambient temperatures and in zero magnetic field, exhibit large-scale magnetic order of their individual electron-spin magnetic moments (ferromagnetism *senso lato*) owing to superexchange interactions at the atomic level. Most magnetic minerals in rocks belong to the iron–titanium oxide system (FeO–TiO_2–Fe_2O_3 ternary system — magnetite, hematite, maghemite, and Ti-rich and cation-deficient phases), or are specific iron sulphides or iron oxyhydroxides. The magnetic properties of these minerals change markedly with composition and grainsize. The important point is that the primary mix, composition, and grainsize of these minerals may not remain stable, but may change with source variation, or over time, owing to secondary chemical, temperature, or pressure effects. These effects can be recorded as a changed magnetic re-

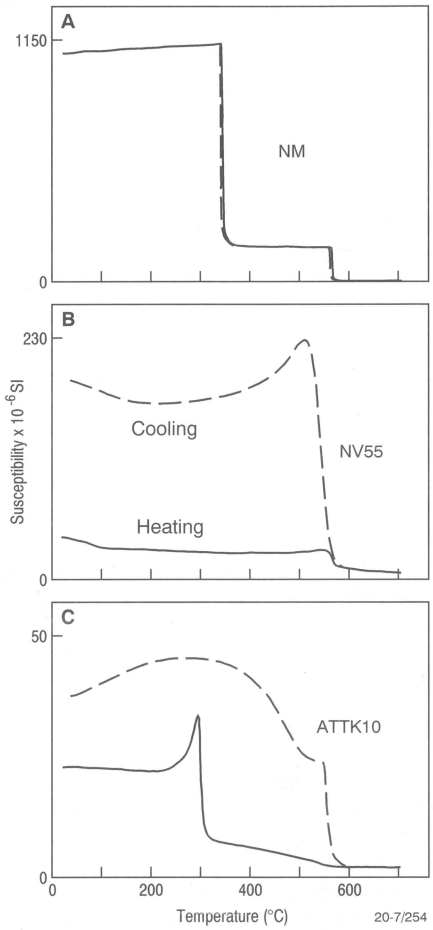

Fig. 7. Thermomagnetic curves (susceptibility/temperature) obtained from the KLY3S kappabridge–CS3 furnace unit for three samples. They span the temperature range 25–700°C, and show various features. (A) Reversible heating–cooling curves (no magnetochemical change) and two well-defined Curie points (sharp drops in susceptibility) indicating nickel (lower temperature drop) and magnetite. (B) Two Curie points (small drops in susceptibility on heating curve) indicating probably hemo-ilmenite (lower temperature) and magnetite. (C) Two Curie points, one well-defined for pyrrhotite (Fe_7S_8), the other a subdued indication for magnetite with some titanium. (B) and (C) show irreversible heating–cooling curves (chemical change during heating): the cooling curve for (B) shows enhancement of magnetite (breakdown of matrix iron-silicates) and so does (C), in which the enhancement is probably due to the decomposition of pyrrhotite.

sponse (e.g., secondary directions of permanent magnetism, enhanced or reduced susceptibility, an anisotropy in susceptibility) and may be of broad geologic and economic significance.

If we understand the source of the magnetic response (permanent and induced) of rocks, we will clearly gain a richer understanding of the geological events (often subtle and undetected by more mainstream methods) that have affected them: we will get more out of the applications, and we can capitalise on the greater level of detail now being returned by more sophisticated data-acquisition instrumentation. To extract robust and competitive interpretations therefore, analysis needs to be underpinned with knowledge of the magnetic properties of the rocks studied: magnetic mineral composition; anisotropy of response; and magnetic grainsize distribution. Magnetic susceptibility is a parameter that can yield much of this information, but, until now, AGSO's capability for measuring it has been only rudimentary.

KLY3S/CS3 spinner kappabridge–furnace system

The kappabridge–furnace system measures very precisely the magnetic susceptibility of rocks, its anisotropy (the degree to which induced magnetisation varies with direction in a sample), and its change with temperature over a wide range of susceptibility values, from the weakest diamagnetic (negative susceptibility) to ore-grade material. It has a sensitivity of 10^{-7} to 10^{-8} SI units. It is autobalancing, autocompensating, and autoranging, and the measurement procedure is designed so that measurements are automatically freed of thermal drift and background. A personal computer controls all aspects of instrument operation, and a sophisticated software package caters for real-time and off-line processing, plotting, and analysis of data.

The anisotropy of magnetic susceptibility (AMS) can be measured either by spinning or by manual orientation of the sample. AMS in a rock indicates that a fabric is present. As a technique for determining fabrics, AMS is extremely sensitive and quick (~3 minutes/sample), and can often reveal fabrics that go undetected using standard, more time-consuming methods. AMS is described by the directions and magnitudes of the maximum, intermediate, and minimum susceptibility axes of the susceptibility ellipsoid, and various shape parameters.

Attaching the CS3 furnace to the kappabridge enables bulk susceptibility (K) to be measured as a function of temperature (T). With the correct experimental procedure and care in interpretation (new magnetic material can be created in response to heating), the K–T thermomagnetic curve is used to make a quick analysis of the magnetic minerals in a sample, and to indicate magnetic grainsize distribution. Samples are in the form of ~0.3–0.5cm^3 of crushed rock. A heating–cooling cycle (25–700°C) takes about 2.5 hours, returns ~500 pairs of susceptibility and temperature measurements, and runs automatically. The planned addition of a low-temperature unit will extend K–T determination to liquid nitrogen temperature and yield additional compositional and grainsize information.

KLY3S/CS3 — typical results

To illustrate the types of information we obtain from the instrument, we present typical results from using it in the two modes: K–T thermomagnetic curves with the kappabridge–furnace system; and AMS (magnetic fabric) with the kappabridge alone.

K–T thermomagnetic curves (Fig. 7)

Reversible heating and cooling curves (Fig. 7A) demonstrate that the magnetic minerals have not undergone magnetochemical change. The sample is a standard and comprises a mixture of nickel and magnetite (Fe_3O_4). The two sharp susceptibility drops define the temperatures at which ferromagnetic (*s.l.*) ordering in the magnetic minerals is thermally broken down. Each of those temperatures is a Curie point (T_c) of one of the minerals present: the Curie point is a fundamental and characteristic property of a magnetic mineral, and we can use its value to identify the mineral species. Here, we have two T_cs: 350°C and 570°C. Knowing that the T_cs of nickel and magnetite are ~355°C and ~575°C respectively, we would conclude from our measured values that those are the two minerals present.

The heating and cooling curves for a sample of the Nungbalgarri Volcanics (~1.72 Ga) from the northwest McArthur Basin (NT) are markedly different (Fig. 7B), indicating that heating has caused substantial magnetochemical change. The heating curve shows two distinct slope changes: a shallow one at ~85°C and a steeper one at ~570°C. It also shows that no detectable magnetochemical change has occurred between 85 and 570°C: K/T is essentially flat. We therefore conclude that the Curie points, indicated by the slope changes, show that two magnetic minerals are present in the sample. The low T_c mineral is most likely hemo-ilmenite (a member of the series $Fe_{2-x}Ti_xO_3$, $0 \leq x \leq 1$, between end members hematite, $x = 0$: T_c ~675°C, and ilmenite, $x = 1$: T_c ~–220°C). The high T_c mineral is a slightly impure magnetite (some titanium in the lattice). The cooling curve indicates that a high T_c (~575°C) mineral formed during heating, in the time the sample spent above 575°C. We interpret it as pure magnetite created from the breakdown of iron-rich silicate matrix minerals. The presence of the pronounced peak just below T_c — the so-called 'Hop-

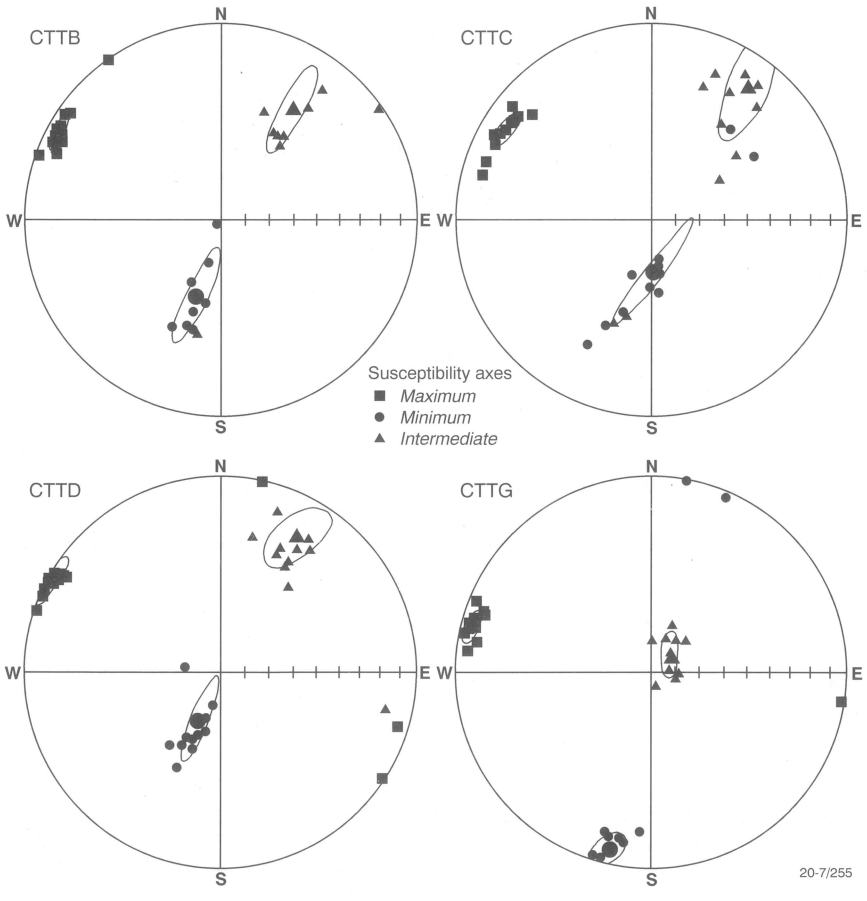

Fig. 8. Anisotropy of magnetic susceptibility for four sites in the Terrica beds, in the southern New England Orogen. The maximum, intermediate, and minimum axes of susceptibility are plotted (with the mean directions and ellipses of 95% confidence) on the lower hemisphere of an equal-area net. The presence of a systematic magnetic fabric oriented WNW–ESE is evident (the plane containing the K_{max} and K_{int} axes), and is in the same direction as the regional tectonic grain of the surrounding Texas beds, implying that the fabric was imposed tectonically.

kinson' peak — further tells us that the new material contains a very fine-grained fraction.

A sample of the Condamine beds (Late Permian) from the Texas block, southern New England Orogen, again has irreversible heating and cooling curves (Fig. 7C) reflecting magnetochemical change. The most prominent features of the heating curve are the sharp drop in susceptibility at ~315°C, the sharp 'Hopkinson' peak before the drop, and a subdued drop at ~550°C. The T_c close to 320°C identifies the main magnetic mineral as monoclinic pyrrhotite, Fe_7S_8 ($\times = 0.125$ in the general pyrrhotite formula $Fe_{1-x}S$, $0 \leq \times \leq 0.13$), and the sharp peak indicates that a very fine-grained fraction is present. The absence of a sharp increase in susceptibility at 220°C and sharp decrease at ~270°C (T_c) rules out the presence of hexagonal pyrrhotite Fe_9S_{10} ($\times = 0.1$), which can coexist as an intergrowth with Fe_7S_8. The T_c at ~550°C points to the subordinate magnetic mineral being titanomagnetite ($Fe_{3-x}Ti_xO_4$, $0 \leq \times \leq 1$), close in composition to magnetite ($\times = 0$). The T_c of titanomagnetite decreases from ~575°C (magnetite) to ~–150°C (ulvöspinel, $\times = 1$) as Ti increasingly substitutes for Fe. At temperatures above its T_c of 320°C, pyrrhotite is unstable and decomposes to magnetite. We see this in the cooling curve: the sharp increase in susceptibility at ~570°C is due to new magnetite formed during heating, in the time the sample was above 570°C.

Anisotropy of susceptibility (magnetic fabric)

The tectonically imposed magnetic fabric (Fig. 8) is an example of the use of AMS as an ancient stress field indicator. Although the magnitude of susceptibility anisotropy is small (1.3%), the maximum, intermediate, and minimum axes of the susceptibility ellipsoids are *directionally* coherent within and between four sites in the Lower Permian Terrica beds (Terrica inlier), indicating that a systematic fabric is present. The plane of this fabric (the plane in which the maximum and intermediate susceptibility axes lie) is aligned WNW–ESE.

This fabric information can be applied to a geological problem: constraining the timing of oroclinal bending of the Texas–Coffs Harbour Megafold, southern New England Orogen. Geological arguments are equivocal: estimates of the time at which bending occurred range from as old as latest Carboniferous (310–300 Ma) to as young as Late Permian (265–255 Ma), and put little emphasis on the duration of bending. Palaeomagnetic studies show that bending was under way by the Early Permian (Sakmarian, 293 Ma), and was concluded some time before ~265 Ma. This is where the fabric information is useful. The regional tectonic grain imposed by megafold deformation of the Carboniferous Texas beds, in which the Terrica inlier is located, is WNW–ESE. Detection of a similarly oriented, WNW–ESE fabric in the Terrica beds shows that the beds have experienced the same stress field. We can therefore further constrain the conclusion of bending to the period postdating the Terrica beds (most probably of Allandale age, within the Early Permian), or ~265 Ma.

Significance to AGSO

With the addition of the KLY3S/CS3 system to other rock magnetic techniques we have available, AGSO's Black Mountain palaeomagnetic laboratory is now on its way to transforming into an applied magnetics (*s.l.*) laboratory, able to partly fulfill AGSO's perceived need to develop a rock properties capability for internal and external clients. Advances in technology for measuring the magnetic parameters of rocks, in data analysis and presentation techniques, and in interpretation processes have opened up new opportunities for magnetic-based methods: the field continues to be a growth area in geoscience endeavour.

[1] Minerals Division, Australian Geological Survey Organisation, GPO Box 378, Canberra, ACT 2601; tel. +61 6 249 9319 (JG), +61 6 249 9324 (CK), fax +61 6 249 9986.

Piercing the regolith veil

Identifying parent rocks from weathered equivalents, Eastern Goldfields, Western Australia

Alastair Stewart[1] & Julienne Kamprad[1]

Geological mapping of Archaean bedrock in the Western Australian goldfields is hampered by a thick regolith of weathered rock and surficial sediments. In the Lake Violet 1:100 000 Sheet area of the highly prospective Yandal greenstone belt, X-ray diffraction (XRD) and portable infrared mineral analyser (PIMA) analyses of weathered rotary air blast (RAB) drilling cuttings have provided a means of identifying felsic, mafic, and ultramafic parent igneous rocks where drilling did not reach unweathered bedrock. The results will yield a solid geological map of Archaean greenstones, an essential first step in gold exploration and prospectivity studies.

Regional mapping is an essential element of mineral exploration, because it reveals the locations, compositions, proportions, metamorphic states, relationships, and structural dispositions of the outcropping rocks. In the northern Eastern Goldfields, Archaean greenstones and granites are deeply weathered, and largely concealed by surficial sediments. Hence, surface regional mapping provides a very incomplete picture of the bedrock. Detailed aeromagnetic surveys reveal magnetised rocks in excellent detail in many areas; however, in rocks lacking magnetic properties, such as some mafic and felsic volcanic and sedimentary sequences, greenstone belt geology and structure remain obscure.

To overcome the problem of deep weathering in the goldfields, RAB drilling evolved as a key step in exploration. Truck-mounted rigs air-drill vertical holes through the regolith, usually to 'blade refusal', where the bedrock is fresh enough to prevent further drilling. The drillers collect samples of the cuttings for assay every metre, and arrange them in order beside the hole. The bottom few cuttings heaps thus provide a sample of nearly fresh bedrock. Spacing of the holes ranges from a kilometre or so to a few metres as gold assays of the cuttings rise, and fill-in drilling proceeds.

Drilling has been extensive in the Lake Violet 1:100 000 Sheet area of the Yandal greenstone belt, where we sampled the bottom heap from RAB holes every 600–800 m to gain a picture of bedrock types and distribution and possibly large-scale structure as well. RAB drilling did not proceed to bedrock everywhere. In these holes, the bottom heap of cuttings is composed of weathered rock, mainly clay. These cuttings were sampled, the minerals in each were identified at AGSO by X-ray diffraction (XRD) and by a portable infrared mineral analyser (PIMA), and a likely parent rock for each weathered assemblage was assigned. Many bedrock samples were also analysed, but suites of samples down a single hole from weathered to fresh rock were not collected. A total of 677 RAB holes was examined (24 per day), and 200 sampled for XRD and PIMA analysis.

This note sets out the rationale used to assign parent rocks (felsic, mafic, or ultramafic) to weathered assemblages, lists some typical weathered assemblages encountered from each parent, and discusses whether the results are reasonable and whether or not the weathered material is *in situ*.

Methods

We used a Siemens model D500 X-ray diffractometer with Cu radiation to identify crystalline minerals, and a PIMA reflectance spectrometer to further identify hydrous minerals, carbonates, and sulphates. Each sample was analysed as a 'whole-rock' on the two instruments. XRD identifications were made by examining peak heights and comparing with standards. PIMA identifications relied on wavelength, intensity, shape of absorption troughs, and comparison with standards in the AusSpec International Spectral Library (1995). The PIMA was particularly useful for distinguishing smectitic clays from chlorite, as XRD peaks for these overlap. Thus, the single trough at 2207 nm distinguished montmorillonite from nontronite, Fe-chlorite, and Mg-chlorite. Likewise, the similar pair

of primary AlOH absorption troughs typical of kaolinite, dickite, and halloysite were distinguished by their contrasting intensities and wavelengths.

No mineral separation, glycolisation, or other techniques were utilised.

Results

The minerals identified, in decreasing frequency of abundance, were (with abbreviations used in Table 2 in brackets): quartz (qz), kaolinite (kln), chlorite (chl), illite (ill), smectite (smec; generally but not always further identified as montmorillonite or nontronite), plagioclase (plag), montmorillonite (mnt), feldspar (feld), epidote (ep), nontronite (ntn), goethite (Fe-ox), actinolite (act), muscovite (musc), serpentine (serp), hematite (hem or Fe-ox), mixed-layer clays (ML - not further identified), talc (tlc), calcite (cc), tremolite (trem), pyrite (py), dolomite (dol), halite (hal), biotite (bt), jarosite (jar), and cryptomelane (crp).

Plagioclase, feldspar, biotite, muscovite, chlorite, epidote, pyrite, actinolite–tremolite, talc, and some serpentine and quartz are unweathered relics of the Archaean parent rocks. Minerals formed by weathering, and their possible parent minerals, are identified in Table 1 (from Righi & Meunier 1995: in Velde, B. (ed.), 'Origin and mineralogy of clays', Springer-Verlag, Berlin, 43–161).

Procedure for assigning a parent rock

The two most common minerals identified were quartz (85% of samples) and kaolinite (in 75%), even in samples in which no quartz had been identified in the field. The quartz in these samples represents silica set free by the weathering of feldspar and, to a lesser extent, pyroxene, amphibole, and mica — minerals that are richer in silica than kaolinite (46.5% SiO_2). (Quartz has not been added to the weathering profile by wind or water-transport because the samples come from tens of metres below ground level, well below surficial sediments.) Hence, quartz is of no use in assigning an initial felsic or mafic identification.

All samples of recognisable felsic rocks, but no recognisable mafic or ultramafic rocks, contain illite [$K(Fe, Mg, Al)_2(Si, Al)_4O_{10}(OH)_2$], and so the presence or absence of illite was used as the initial criterion for respectively assigning a felsic or mafic parent.

The procedure for assigning a parent rock can be arranged in a flow chart (Fig. 9).

Partly weathered samples contained some clay, and these were useful for interpreting the completely weathered samples. In addition, all possible field observations on a sample — such as grainsize, presence or absence of discrete grains (recognised optically or dentally) or phenocrysts and their size, relict texture and structure, and colour — were used to augment the XRD and PIMA data. Many sampled cuttings heaps, however, consisted of featureless loose clay or clay-rich powder.

A felsic rock can be so intensely weathered that illite has changed to kaolinite, but in this case a silicic rock should retain discrete quartz grains detectable in the field. An intensely weathered intermediate rock, containing no primary quartz, could be misassigned a mafic parent.

Table 2 lists some typical mineral assemblages encountered and their assigned parent igneous rocks. Full lists of all assemblages from the Lake Violet 1:100 000 Sheet area are available from the authors.

Cuttings samples of recognisably sedimentary origin (from bedding lamination) tend to contain clay assemblages which are identical with felsic igneous assemblages. Observations such as texture and structure are needed to distinguish a felsic igneous from a sedimentary parent.

Table 1. Minerals formed by weathering and their possible parent minerals

Minerals formed by weathering	*Possible parent minerals*
Kaolinite	Alkali feldspar, plagioclase, mica, illite, smectite
Illite	Alkali feldspar, muscovite
Smectite (undivided, montmorillonite, nontronite)	Ca-plagioclase, feldspar, mica, chlorite, amphibole, pyroxene, olivine, serpentine
Fe-oxides	Biotite, amphibole, pyroxene, spinel
Secondary quartz	Released during weathering of above

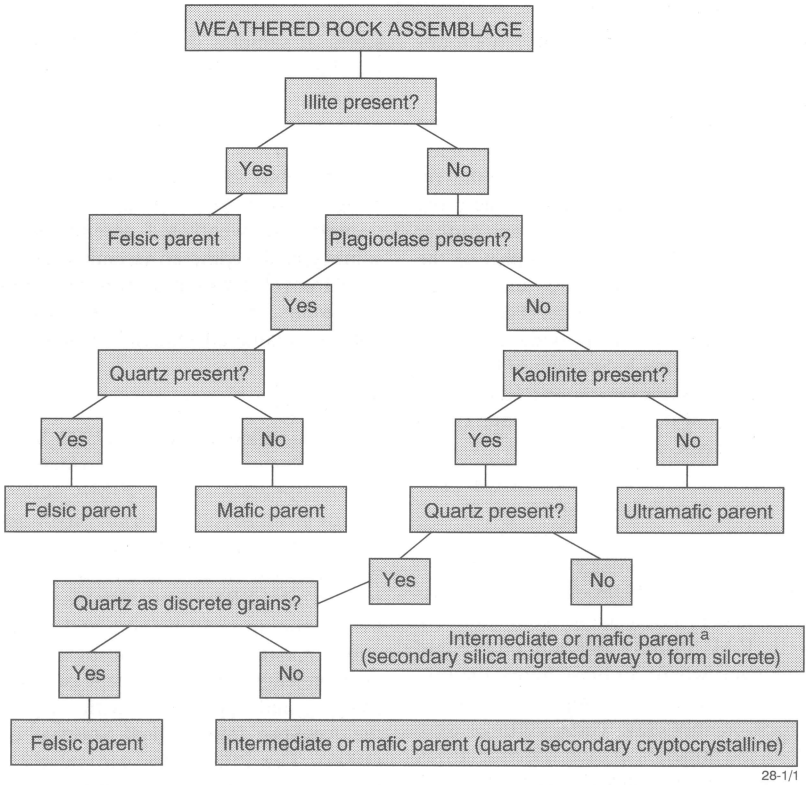

Fig.9. Flow chart for assigning a parent rock to a weathered rock assemblage.

Discussion

Are the results reasonable?

At first sight, to ignore quartz as a criterion for felsic or mafic parentage seems a drastic step, but as it occurs in 85 per cent of assemblages, including some that are of recognisably mafic or ultramafic parentage from textural evidence, it is not diagnostic. Nevertheless, the results are reasonable because the assemblages contain clays and other minerals that were not used for diagnosis, but which can be expected to occur in the weathered equivalent of the assigned parent. Thus:

- chlorite is present in thirteen out of sixteen ultramafic assemblages.
- talc occurs almost exclusively in ultramafic assemblages.
- Fe-oxides are noticeably more common in mafic assemblages than in felsic ones.
- muscovite is absent from mafic and ultramafic assemblages.
- serpentine is virtually absent from felsic assemblages.
- montmorillonite and quartz are virtually absent from ultramafic assemblages (secondary silica having migrated away), although nontronite (iron-rich smectite) is commonly present.

It should be borne in mind, however, that muscovite (and biotite) can form by hydrothermal alteration of mafic rocks in the

[a] Use other criteria to distinguish intermediate from mafic. In Eastern Goldfields, intermediate rocks are typically feldspar-phyric volcanics, whereas mafic rocks are typically equigranular.

vicinity of gold lodes (Phillips & Groves 1983: Journal of the Geological Society of Australia, 30, 25–39), and that chlorite and talc commonly form during shearing of mafic rocks.

Are the clay assemblages in situ?

In the Yandal greenstone belt, the surficial components of the regolith — such as colluvium, laterite, sand, and playa-lake deposits — are certainly transported. However, the deeper parts of the regolith (i.e., the saprolite and sap rock) are likely to be in situ, for two reasons: firstly, the weathered assemblages of the three igneous groups are markedly and consistently different, and so are unlikely to have been mixed together; and, secondly, although the data are not yet plotted on a map, preliminary examination of them indicates that assemblages tend to form well-defined groups of one or closely related types, which change suddenly to another type. The sudden change suggests a lithological boundary, and thus further supports the assertion that the weathered assemblages are in situ.

Table 2. Typical assemblages[b] in weathered igneous rocks

Felsic parent									
qz	+	feld	+	kln	+	ill			
qz	+	feld(tr)	+	kln?	+	mnt	+	ill	
qz grains[c]	+	kln							
qz	+	kln	+	ill					
qz	+	plag	+	chl	+	ill	+	smec	
qz	+	plag	+	kln	+	mnt	+	ill	+ smec
Mafic parent									
kln	+	chl	+	smec	+	act	+	ntn?	
qz[d]	+	kln							
qz	+	kln	+	chl	+	ep?			
qz	+	kln	+	Fe-ox					
qz	+	kln	+	mnt	+	smec			
qz[e]	+	plag	+	chl	+	smec	+	ep?	+ act
qz	+	plag	+	kln	+	chl	+	smec	
Ultramafic parent									
chl	+	act	+	serp?	+	qz?(tr)	+	ntn?	+ smec
chl	+	act	+	tlc					
chl	+	smec	+	act	+	ep?			
chl	+	smec	+	trem	+	mnt?			

[b] Query signifies detected, but identification is possible only; tr = trace.
[c] Identified in field.
[d] Cryptocrystalline secondary; identified by XRD only; formed during weathering of parent minerals to kaolinite.
[e] Minor; could have formed during weathering of mafic mineral to smectite.

Conclusion

Together with textural, structural, and granularity observations of Archaean weathered greenstones, and some reasonable assumptions on the origin of illite, kaolinite, and quartz, XRD and PIMA analyses have produced a scheme for assigning felsic, mafic, or ultramafic parentage to the weathered assemblages. Future work will involve plotting the parent rocks on the Lake Violet 1:100 000 map, and then using the map for structural and prospectivity studies.

Acknowledgments

Colin Pain, David Tilley, Ivor Roberts, and Chris Cuff reviewed and significantly improved the manuscript. Tony Eggleton and Bob Gilkes provided early assistance.

[1] Minerals Division, Australian Geological Survey Organisation, GPO Box 378, Canberra, ACT, 2601: tel. +61 6 249 9666 (AS), +61 6 249 9274 (JK); fax +61 6 249 9983; e-mail astewart@agso.gov.au, jkamprad@agso.gov.au.

Pieces of eight

Charting the event-related surfaces of the Mount Isa and McArthur basins

Peter N. Southgate[1], Steve Abbott[2], Barry E. Bradshaw[1], Jan Domagala[3] M. Jim Jackson[1], Andrew A. Krassay[1], John Lindsay[1], Bruce A. McConachie[1], Rod Page[1], Terry Sami[4], & Allan T. Wells[5]

AGSO, the Northern Territory Geological Survey, and the Geological Survey of Queensland are using the concepts of sequence stratigraphy to identify chronostratigraphic surfaces within the Mount Isa–McNamara–Fickling–McArthur–Nathan Groups of the Palaeoproterozoic McArthur and Mount Isa basins. These surfaces facilitate correlation within and between the respective groups, and are thus providing a mechanism for establishing a time-series predictive tectonostratigraphic framework for Palaeoproterozoic basin evolution, one of the objectives of the collaborative NABRE ('North Australian basins resource evaluation') project.

Integrating the results of SHRIMP zircon dating, palaeomagnetic studies, and sequence analysis of gamma-ray curves and facies-stacking patterns distinguishes eight event-related surfaces (A–H) and their respective accommodation packages (1–7; Fig. 10).

Basin initiation, represented by **surface A**, occurred at about 1660 Ma (youngest dates from detrital zircons in the Torpedo Creek Quartzite). Both paraconformable and unconformable geometric relationships occur across surface A.

Surface B is most pronounced in the lower Gunpowder Formation at Crocodile Waterhole (Mammoth Mines 1:100 000 Sheet area) and adjacent to the Fiery Creek Fault at Mellish Park (Mount Oxide Sheet area). In both areas, it is overlain by a conglomerate which fines laterally over a short distance and is replaced by a coarse-grained pebbly sandstone.

In the Kamarga region, an interval of sulphate evaporite pseudomorphs in the middle of the Gunpowder Formation records a basinward shift in facies associated with the tectonic event recorded by surface B. Base-metal sulphides are associated with these evaporites. Higher-order accommodation cycles found above and below surface B display markedly different stacking patterns, indicating that accommodation and sediment supply rates changed across this boundary.

In the McArthur region, the surface is marked by a pebbly sandstone in otherwise fine-grained silty sediments of the Mallapunyah Formation. The pebbles are derived from the Tawallah Group, consistent with a basinward shift in facies at this surface.

In the McNamara and Mount Isa Groups, **surface C** marks the switch from gradually declining accommodation rates in the Paradise Creek Formation and lower Moondarra Siltstone to increasing rates in the Esperanza Formation and upper Moondarra Siltstone. In the McArthur region, the event that produced this surface coincided with the demise of the Amelia Dolomite carbonate ramp and the rapid influx of clastic sediments of the Tatoola Sandstone. The Australian apparent polar-wander path (APWP) records a bend at this time, suggesting that a tectonic event led to these changes.

An angular truncation beneath **surface D** is apparent on seismic sections from the Bowthorn region. In outcrop, this surface probably occurs somewhere in the Lady Loretta Formation. The pronounced basinward shift in facies evident from the gamma-ray log in the middle of the Native Bee Siltstone in the Mount Isa valley probably records this event. Along the southern flank of the Mur-

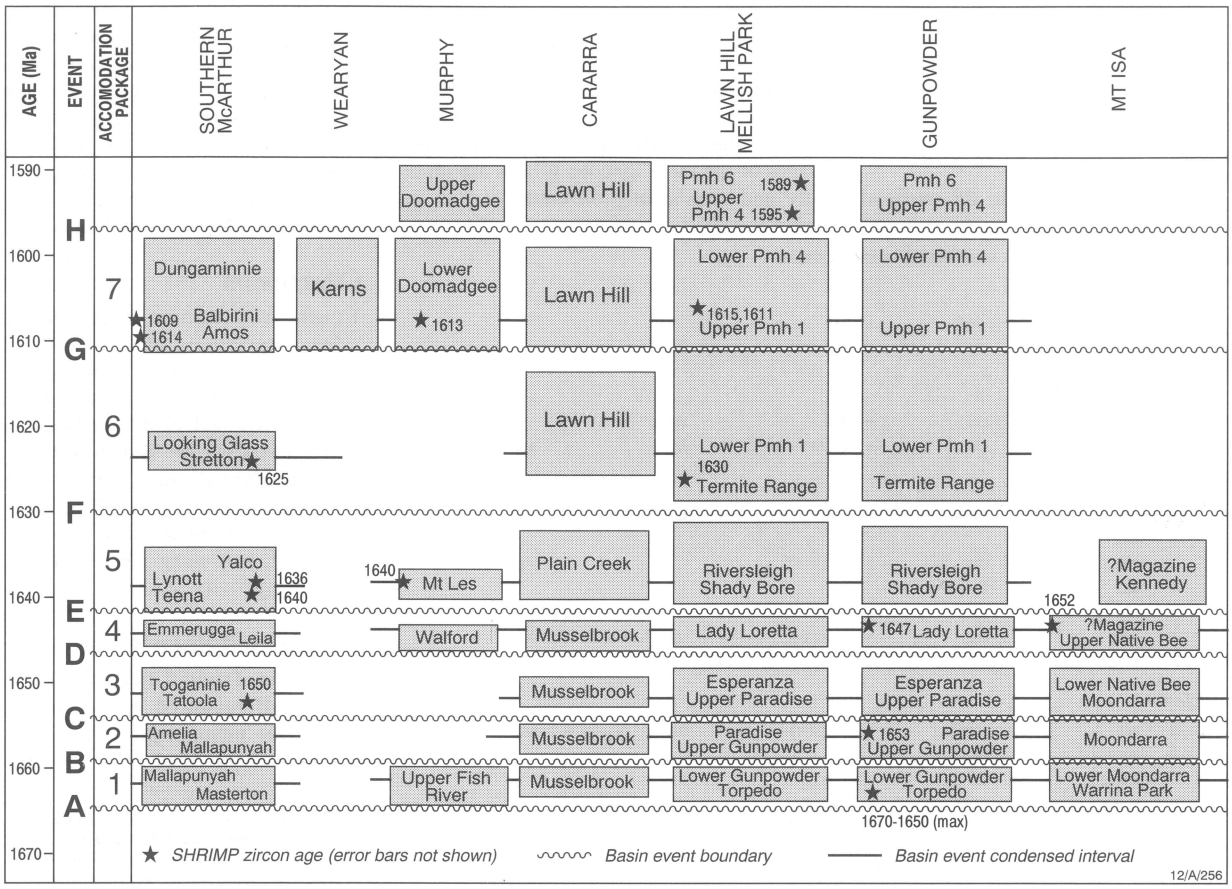

Fig. 10. An event chart for the southern McArthur to Mount Isa region.

phy Inlier, surfaces B, C, and D amalgamate at the base of the Walford Dolomite. In the southern McArthur area, sandstone and calcareous sandstone of the Leila Sandstone rest with sharp contact on the Tooganinie Formation. The Tooganinie Formation displays gradually decreasing accommodation rates, whereas the overlying Leila, Myrtle, and Emmerruga units display gradually increasing accommodation rates. Surface D may record the initial transmission of intraplate stresses associated with a hairpin bend on the APWP curve.

Surface E records a major reorganisation of the Mount Isa and McArthur basins. On sesimic sections, reflectors display truncation and onlap relationships below and above this surface respectively. In the Lawn Hill–Riversleigh region, sandstone and conglomerate of the Shady Bore Quartzite record a change in provenance, and overlie a prominent incision surface with associated incised valleys at or near the base of this formation. Surface E also records the switch from carbonate depositional systems of the lower McNamara Group to the clastic-dominant systems of the upper McNamara Group. In the McArthur region, surface E coincides with the development of small strike-slip basins of the Teena, Barney Creek, and Reward depositional systems. A prominent hairpin bend on the APWP curve spans this interval. Intraplate stresses associated with the tectonic event responsible for the hairpin bend probably led to basin reorganisation across surface E.

Sandstone deposits of the Termite Range Formation record relative uplift of and sediment influx from a northwestern provenance. On the Wearyan Shelf, mixed carbonate and siliciclastic deposits of the Karns Dolomite (probably deposited during the final phases of Lawn Hill Formation time) overlie sandstone of the Tawallah Group. Erosion of possibly lower McArthur Group as well as Tawallah Group rocks probably took place in response to this uplift. Hence **surface F** records a marked basinward shift in facies in the Lawn Hill region, and uplift and erosion on the Wearyan Shelf. SHRIMP zircon dates from the Lynott Formation and Stretton Sandstone in the McArthur Group imply that about 11 m.y. of time is missing, suggesting that erosion probably extended into the McArthur region at this time.

In the southern McArthur region, **surface G** records a marked angular unconformity at the base of the Nathan Group. Along the southern flank of the Murphy Inlier, the surface at the base of the Doomadgee Formation incises the underlying Mount Les Siltstone, and marks the region where surfaces F and G amalgamate. Farther south, surface G is associated with seismic truncation, and is correlated with the base of a pronounced shift to the left in the gamma log in unit Ɐmh 1 of the Lawn Hill Formation. This change in gamma-ray signal marks a basinward shift in facies and the influx of coarser-grained tubiditic sandstone possibly derived from erosion of the Wearyan Shelf.

On seismic sections, **surface H** is characterised by truncation. Fault movement associated with this event is responsible for the formation of small fault-bounded basins or local depocentres. The Century deposit probably occurs in one of these smaller depocentres.

[1] NABRE Research Team, Minerals Division, Australian Geological Survey Organisation, GPO Box 378, Canberra, ACT 2601; tel. +61 6 249 9206 (PNS), +61 6 249 9413 (BEB); fax +61 6 249 9956; e-mail psouthga@agso.gov.au, bbradsha@agso.gov.au.
[2] Northern Territory Geological Survey, GPO Box 2901, Darwin, NT 0801; tel. +61 8 8999 5307; fax +61 8 8999 6824; e-mail sabbot@dme.nt.gov.au.
[3] Geological Survey of Queensland, GPO Box 194, Brisbane, Qld 4001; tel. +61 7 237 1503; fax +61 7 235 4074; e-mail dme@mailbox.uq.oz.au.
[4] Department of Geological Sciences, Queen's University, Kingston, Ontario K7L 3N6, Canada; tel. +1 613 545 6170; fax +1 613 545 6592; e-mail samit@dna.ca.
[5] c/o NABRE Research Team, Minerals Division, Australian Geological Survey Organisation, GPO Box 378, Canberra, ACT 2601.

Balanced petrology of the crust in the Mount Isa region

Alexey Goncharov[1], Shen-Su Sun[1], & Lesley Wyborn[1]

Refraction/wide-angle seismic data recorded by the Australian Geodynamics Cooperative Research Centre along the Mount Isa geoscience transect (Goncharov et al. 1996: AGSO Research Newsletter 24, 9–10) offer scope for modelling the petrological composition of the crust in this region. Despite considerable lateral variation in seismic velocity distribution at the upper- to lower-crustal levels, the average seismic velocity–depth functions from different parts of the region converge above the Moho, thus indicating that there is a balance of high and low seismic velocities along any vertical profile through the crust. Petrophysical modelling translates this remarkable observation into petrological models, whereby the proportional distribution of felsic, intermediate, and mafic rock in the crust of the Mount Isa Inlier is also balanced.

Velocity model of the crust

The seismic velocity distribution derived from the refraction/wide-angle seismic data along the Mount Isa transect (Fig. 11) varies considerably. It reveals no sharp velocity boundary between the crust and mantle. Instead a thick (up to 15 km) transitional zone exists at 40–55 km depth. Low-velocity layers are quite common both in the crust and in the crust–mantle transition zone. A high-velocity (6.9–7.3 km s^{-1}) body in the middle crust at the centre of the line is an important feature of the model (Goncharov et al. 1996: op. cit.). Although this high-velocity body distinguishes the Mount Isa Inlier from other Proterozoic regions, high seismic velocities at mid-crustal level are not unusual in seismic models for younger extended and rifted continental crust. The seismic P-wave velocity values at greater depths (25–45 km) in Mount Isa are systematically lower than in other Australian Proterozoic and Archaean average models. They are also lower than in global average models and average models for shields and platforms.

Balance of high and low seismic velocities in the crust

A balance of high- and low-velocity rocks along any vertical profile through the crust in the Mount Isa region is apparent in the original seismic velocity model. The best characteristic to quantify this observation is average velocity (i.e., the ratio of the depth to the vertical travel time of seismic energy to that depth). The average seismic velocity–depth functions computed for different parts of the Mount Isa refraction line converge with depth, and form a single trend above the Moho (Fig. 12), thus giving a measure of how high and low seismic velocities balance through the crust.

Another example of such a balance is apparent in the interpretations of the 600-km Tennant Creek–Mount Isa refraction traverse (Fig. 11), from which Finlayson (1982: Journal of Geophysical Research, 87, B13, 10569–10578) derived two one-dimensional seismic models — one for Tennant Creek to Mount Isa and the other for the reverse direction. The average velocity–depth functions calculated from these original seismic models vary appreciably within the top 10–15 km of the crust, but they merge sharply at greater depth and coincide at 35 km (Fig. 12). Both these average velocity–depth curves become practically indistinguishable from the Mount Isa 1994 representative curves from a depth of 45 km, which is above the shallowest Moho position in the region — at about 50 km.

These results are also consistent with the data collected in the Baltic Shield by different seismic methods, including deep seismic-sounding profiles, and vertical seismic profiling in the Kola Super Deep Bore Hole (Fig. 12). The width of the domain in which average seismic velocity values fall obviously narrows with depth (Fig. 12), and we suggest that the results which we have for a large part of the north Australian craton and for the Baltic Shield form parts of some global trend of the average seismic velocity variation with depth in the Precambrian crust (Table 3).

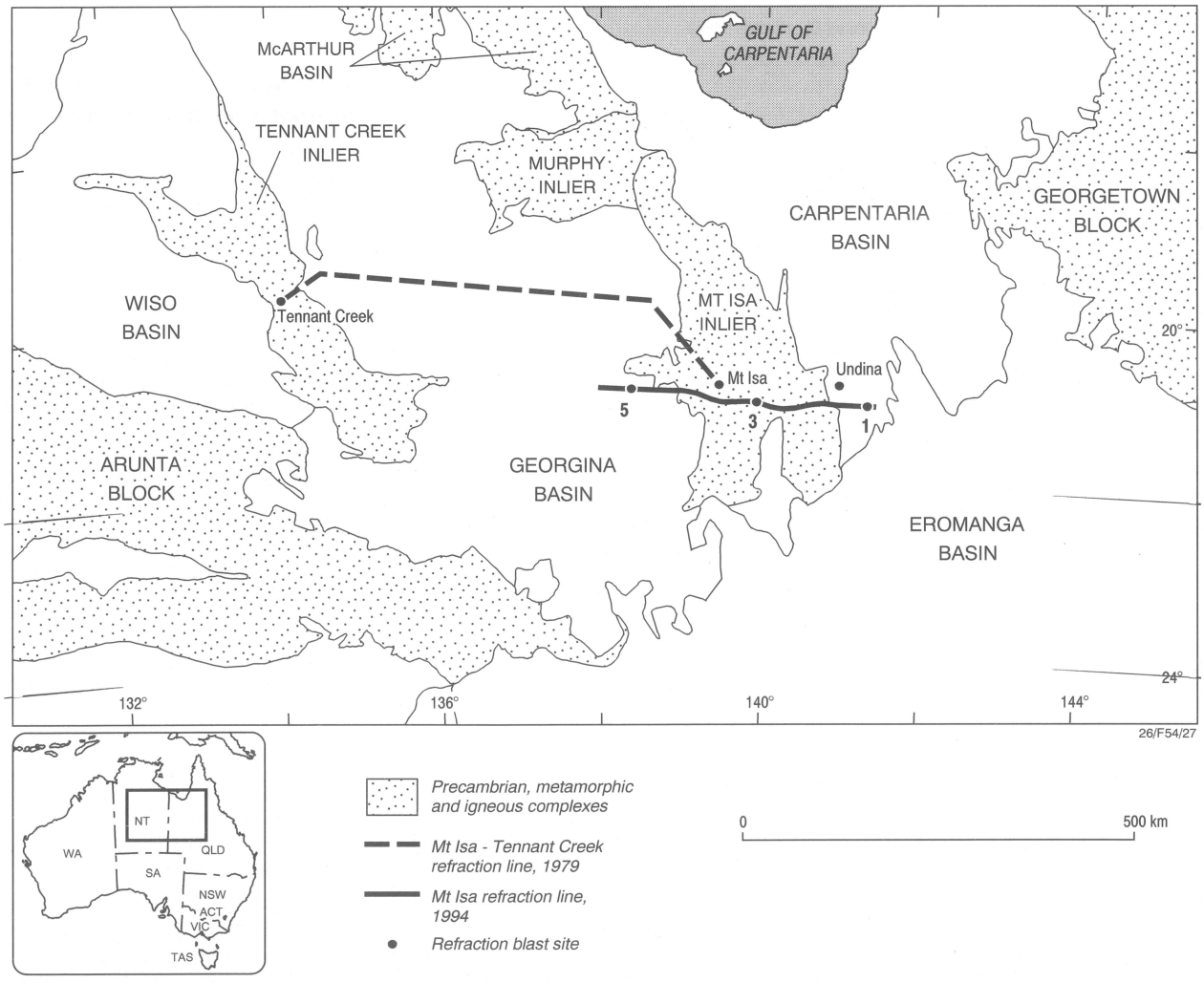

Fig. 11. Tectonic provinces and locations of refraction lines in the Mount Isa–Tennant Creek region.

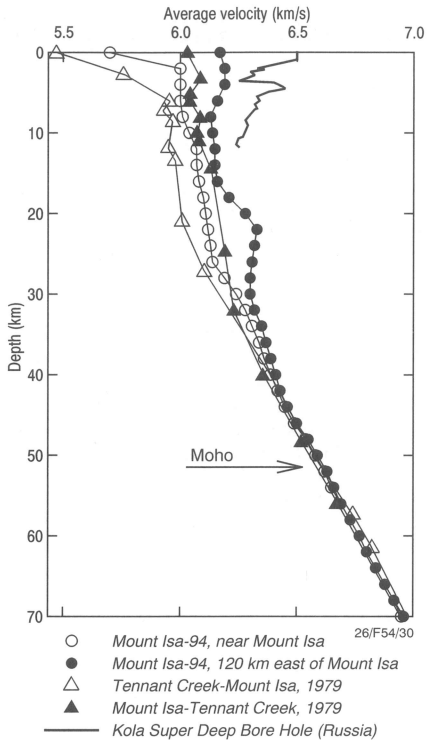

Fig. 12. Average velocity–depth functions calculated for the Mount Isa and Mount Isa–Tennant Creek refraction lines and the Kola Super Deep Bore Hole (Russia).

Is the Osborne ultramafic rock an indicator of the composition of the mid-crustal high-velocity anomaly?

Any high-velocity rock that crops out at the surface is a potential indicator of the petrological composition of a high-velocity body at mid-crustal level. For the Mount Isa Inlier high-velocity body, regionally metamorphosed amphibole peridotite at the Osborne mine, 100 km south of the 1994 refraction line, is such a candidate. Geochemical analysis (trace-element geochemistry in particular) of a sample of this rock showed a high level of crustal contamination, probably related to mineralising events in the region. Consequently a link of this sample to its potential source deeper in the crust or mantle cannot be well constrained.

For the same reason, the tectonic setting in which this rock was generated is also not well constrained. Ultrasonic velocity measurements of this sample at the Research School of Earth Sciences, Australian National University, showed that the P-wave velocity in the sample at room temperature is less than 7 km s^{-1} for a whole range of pressures (0 to 500 MPa). This is considerably lower than that expected for a genuine ultramafic rock. As further petrophysical modelling showed, various spinel lherzolites, for example, have seismic velocities higher than 8 km s^{-1} at room temperature. Severe hydration of the Osborne ultramafic sample might explain its reduced seismic velocity.

The general impression of these results is that the sample cannot constrain the petrological interpretation of seismic velocities.

Table 3. Range of average seismic velocity variation as a function of depth in the Precambrian crust studied

Depth km	*Minimum average volocity km s^{-1}*	*Maximum* average volocity km s^{-1}*
0	5.50	6.50
5	5.91	6.38
10	5.95	6.27
15	5.99	6.24
20	6.00	6.33
25	6.07	6.31
30	6.16	6.30
35	6.27	6.37
40	6.39	6.39
45	6.49	6.49
50	6.57	6.57
55	6.70	6.70
60	6.78	6.78
65	6.87	6.87
70	6.96	6.96

* Note that minimum and maximum average velocity values converge at a depth of 40 km, and form a single trend farther downwards. Minimum average velocity values are taken from the Tennant Creek–Mount Isa data. Maximum average velocity values in the depth range 0–12 km are taken from the Kola Super Deep Bore Hole data; those in the depth range 20–40 km — from the middle part of the Mount Isa 1994 refraction line; maximum average velocity values in the depth range 12–20 km were derived from the extrapolations, and are not well constrained.

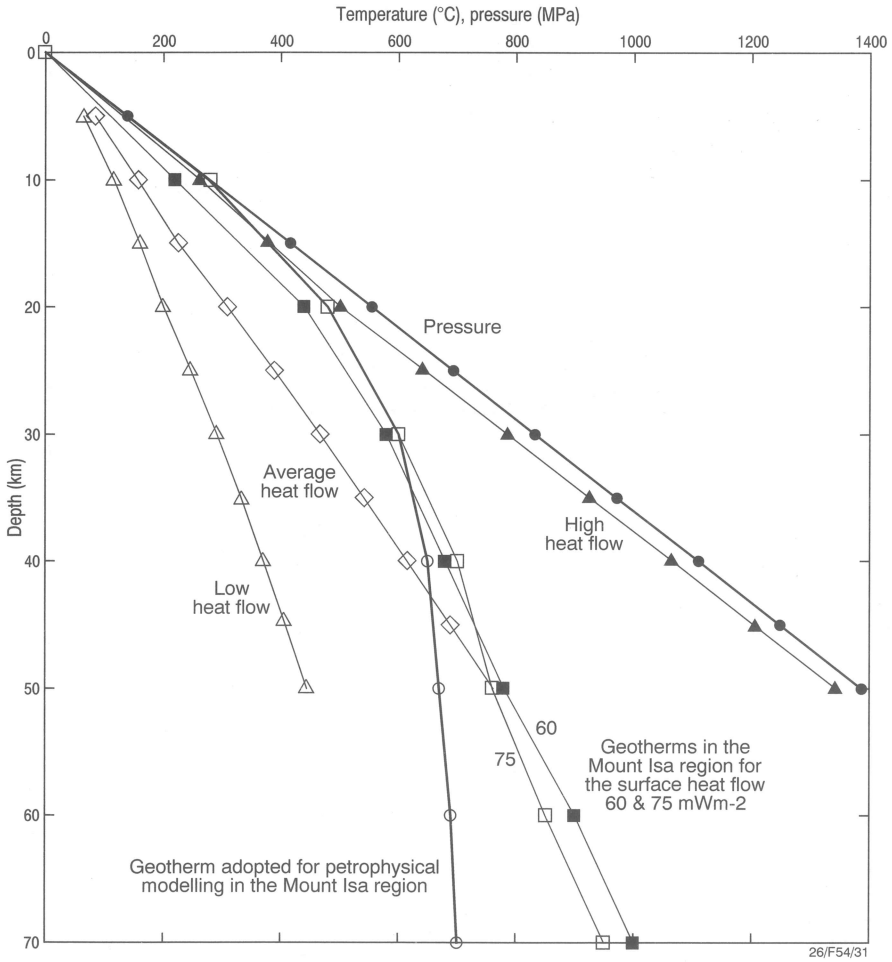

Fig. 13. Pressure and temperature in the crust of the Mount Isa Inlier compared to the regions of low, average and high heat flow as defined by Christensen & Mooney (1995: op. cit.). The Mount Isa geotherms for the surface heat flow of 60 and 75 mW m^{-2} after Cull (1991: op. cit.).

Modelling of mineralogical composition and seismic-wave velocities

Petrophysical modelling developed by Sobolev & Babeyko (1994: Surveys in Geophysics, 15, 515–544) computes intrinsic (crack- and pore-free) elastic properties of the rocks and their temperature and pressure derivatives. This methodology was applied to interpret the Mount Isa velocity model in terms of the likely petrological composition of the crust.

Petrophysical modelling involves an estimation of the PT conditions in modern crust. The pressure–depth function (Fig. 13) was computed for an assumed mean crustal density of 2.830 t m^{-3}, a global average for the continental crust (Christensen & Mooney 1995: Journal of Geophysical Research, 100, B7, 9761–9788). Acceptance of geotherms suggested for different values of the surface heat flow in the Mount Isa region by Cull (1991: Geological Society of Australia, Special Publication 17, 147–155; Fig. 13) makes upper-mantle velocities derived from the refraction data hard to interpret: they appear to be higher than in any rock analysed on the basis of the petrophysical modelling. They also cannot be matched by any of the lithologies represented in the latest compilation of laboratory measurement data (Christensen & Mooney 1995: op. cit.). This problem can be overcome if lower temperatures are adopted for the lower crust and upper mantle in the region (Fig. 13). This modification of geotherms is consistent with the shallow highly radioactive granites in the eastern part of the inlier being responsible for the high heat flow of the upper crust. The geotherm adopted for the petrophysical modelling in the Mount Isa region (Fig. 13) shows an unusually low temperature increase — only 100° — in the depth range from 30 to 70 km.

The temperature gradient in this depth range can be increased to more commonly accepted values (Cull 1991: op. cit.; O'Reilly & Griffin 1985: Tectonophysics, 111, 41–63) at the expense of restricting anomalously high temperatures to the top 10–15 km of the crust. This has to be resolved by further studies.

Intrinsic P-wave velocities were computed for several groups of rocks of different bulk geochemistry and mineralogical composition represented by end-member rock types (Fig. 14). These computations provide a key to translating seismic velocities into petrological models that characterise the bulk geochemistry of the crust. Correlation between seismic velocities and rock petrology is not unique; thus, velocities of 6.1–6.5 km s^{-1} mostly correspond to various granite minerologies but can also apply to diorites (domain A, Fig. 14). This means that a rock with a lower seismic velocity is not necessarily a more felsic rock, so only a probabilistic approach can be used to derive petrological models from seismic velocities.

Two one-dimensional velocity models (Fig. 15) characterising the main features of the original two-dimensional velocity model were interpreted in terms of bulk geochemistry of rocks at different depths predicted by the petrophysical modelling (Fig. 14). Most layers in the resulting petrological models (Fig. 16) are characterised by a probabilistic proportion of rock of different bulk geochemistry. Seismic velocities in some layers are too low to be explained by intrinsic properties of analysed anhydrous magmatic rocks (Fig. 16). An assumption of granite bulk geochemistry for these layers enabled their SiO_2 contents to be estimated. Cracks and pores may explain the low seismic velocities in these layers; this is in qualitative agreement with the wide and numerous north–south oriented faults which disrupt the integrity of the inlier's upper crust. Alternatively, the upper crust might comprise low-grade metasediments; this option is a subject for further studies.

A broad range of rocks of gabbro–diorite bulk geochemistry can explain the high-velocity mid-crustal anomaly (model for anomalous middle part of the inlier, Fig. 16). An important conclusion is that the high-velocity anomaly cannot correspond to ultramafic rock, even under high temperatures at this depth (Fig. 14).

Another important conclusion is that, despite the ambiguity of the velocity–petrology correlation, a balance of high and low seismic velocities along any vertical profile through the crust does translate into petrological models in which the proportional distribution of felsic, intermediate, and mafic rocks in the crust of the Mount Isa Inlier is also balanced. Qualitatively this conclusion can be derived from an analysis of the SiO_2–depth variation: there is a noticeable compensation for less felsic rock in the anomalous-middle-part model at the mid-crustal level by the more felsic rock underneath (Fig. 16). Analysis of SiO_2 contents averaged in an expanding depth-range window (Fig. 16) clearly shows that the whole-line-average and anomalous-middle-part curves merge to less than 1 per cent difference at a depth of 45 km (about 10 km above the Moho), whereat the two models become indistinguishable.

Petrological models in a tectonic context

The Early to Middle Proterozoic tectonic history of the Mount Isa region indicates that numerous ensialic rifting events preceded the Isan Orogeny, and that some of the rifting might have been close to creating new oceanic crust. The presence of high-velocity rocks, interpreted to be intermediate or mafic in nature, within the middle crust supports an extensional regime. Regional extension is normally associated with a raised geothermal gradient, partial melting in the upper mantle, and the creation of weakened zones along which melts are emplaced to a higher level in the crust. Hence direct magmatic emplacement is a viable model for the high-velocity body imaged in the mid-crust. Alternatively crustal shortening during the Isan Orogeny, which thickened the previously thinned crust back to high continental values, may have also thrust some of the lower-crustal mafic rocks to mid-crustal levels. Results presented herein are more consistent with the first option because they imply some kind of crustal melting and fractionation during which lower crust underneath the high-velocity body might have been depleted in its mafic component.

Petrological models in the context of the igneous rocks of the Mount Isa Inlier

At least 25 per cent of the exposed rocks in the Mount Isa Inlier are either mafic or felsic igneous; there are no major suites of intermediate igneous rocks. Each magmatic episode in the inlier is either bimodal or mainly mafic, supporting the interpretation of a mostly extensional regime during the emplacement of these igneous rocks (Wyborn et. al. 1988: Precambrian Research, 40/41, 509–541). The mafic rocks are largely tholeiitic. In the eastern Mount Isa Inlier, the tholeiites of the Soldiers Cap Group are very Fe-enriched. Fe-enriched tholeiites are believed to have formed as a result of extreme fractionation from a high-level magma chamber in the crust (Williams in press: Australian Journal of Earth Sciences). Such a magma chamber may be what the Mount Isa refraction survey has revealed.

Not only are mid-crustal high-velocity bodies rare in the Proterozoic but Fe-enriched tholeiites are rare in the Proterozoic of Australia, having been noted in only two other areas — Broken Hill and Georgetown. However, there are no seismic refraction data available from the Broken Hill and Georgetown areas to check for similar mid-crustal high-velocity layers.

Although the rocks emplaced during the Mount Isa Inlier's major felsic magmatic episodes have notable compositional differences, to a great extent they evince three similar features:

- most are more felsic than 65 wt % SiO_2 and are classified as I- (granodiorite) type (Chappell & Stephens 1988: Transactions of the Royal Society of Edinburgh, 79, 71–86; Wyborn et al. 1992: ibid., 83, 201–209);
- most are derived from sources in which plagioclase is stable (Wyborn et al. 1992: op. cit.); and
- all have Sm–Nd model ages up to 1000 m.y. older than their ages of intrusion.

These features imply that the rocks were derived from pre-existing plagioclase-bearing lower crustal sources, which must have been immense to have generated the huge volume of felsic igneous rocks in the Mount Isa Inlier. I- (granodiorite) types are believed to be generated by partial melting of pre-existing sources of more mafic rocks of tonalite

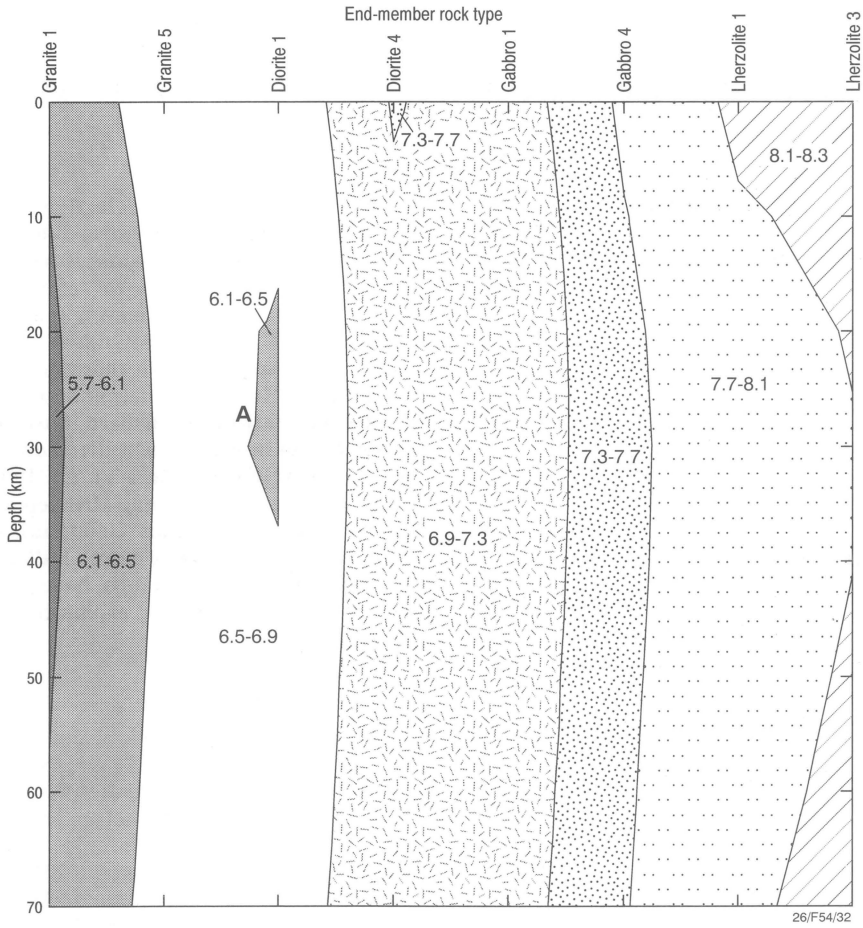

Fig. 14. Intrinsic compressional-wave velocities computed for the Mount Isa PT conditions. Bulk geochemical composition within each group of rocks (granites, diorites, etc.) is similar, but mineralogical compositions within each group (granites 1 to 5, diorites 1 to 4, etc.) vary. Mineralogical composition is controlled by the PT conditions which existed at the time of rock equilibration, and elastic properties of the rock increase with pressure of equilibration owing to mineral reactions changing mineral assemblages from plagioclase-bearing and garnet-free to garnet-bearing and plagioclase-free.

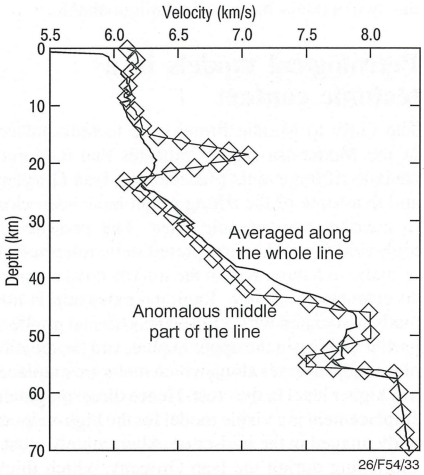

Figure 15. One-dimensional velocity models of the Mount Isa 1994 refraction line which were subjected to petrological interpretation from petrophysical modelling.

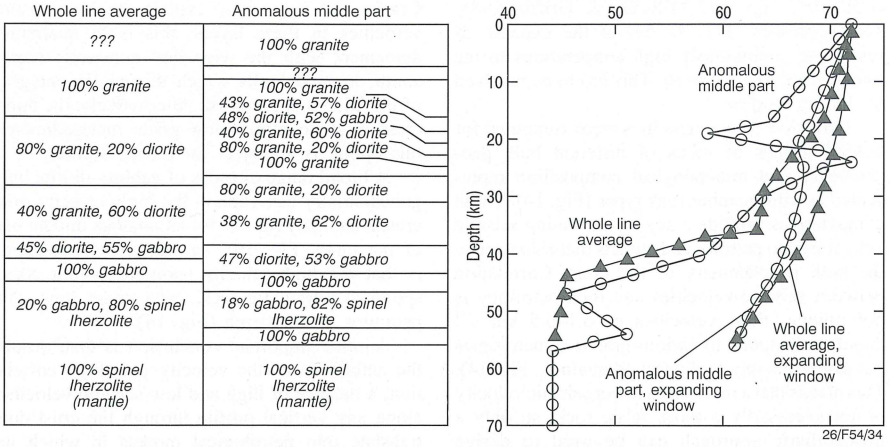

Figure 16. Petrological models of the crust of the Mount Isa Inlier and SiO_2 distribution in the crust. ??? — seismic velocities in these layers cannot be explained by intrinsic properties of analysed anhydrous magmatic rocks. Models represent bulk geochemistry of the rock rather than specific mineralogical composition. The top of the expanding depth-range window used to average SiO_2% was always at 0 km, but the bottom of the window was gradually shifted downwards; averaged values are plotted against the depth of the bottom of this window.

to diorite composition (Chappell & Stephens 1988: op. cit.). The dioritic to gabbroic petrological composition determined for the lower crust in the Mount Isa Inlier (Fig. 16) is in keeping with the inferred origin of the granites: such a source would have contained abundant plagioclase and been in the approximate compositional range to generate I-(granodiorite) type granites. Further, some of the gabbros inferred to exist from the interpretation of seismic velocities might represent the more mafic, denser residues after partial melting of dioritic rocks had generated the abundant felsic igneous rocks.

Acknowledgment

Anthony Budd reviewed the manuscript. We thank him for useful comments.

[1] Minerals Division, Australian Geological Survey Organisation, GPO Box 378, Canberra, ACT 2601; tel. +61 6 249 9595 (AG), +61 6 249 9484 (S-sS), +61 6 249 9489 (LW); fax +61 6 249 9971; e-mail agonchar@agso.gov.au, ssun@agso.gov.au, lwyborn @agso.gov.au.

Rocks of Mount Isa Group age in the Eastern Fold Belt

Rod Page[1, 3] & Tyler MacCready[2, 3]

The eastern and central parts of the Mount Isa Inlier have many structural and stratigraphic complexities. Zircon U–Pb SHRIMP geochronology is helping to resolve some of them — particularly those in the area imaged by the Mount Isa geodynamic transect (Goleby et al. 1997: Abstracts, Geodynamics and Ore Deposits Conference, Australian Geodynamics Cooperative Research Centre, Ballarat, Victoria, 38–41). New isotopic results reported here will help to revise the chronostratigraphic framework of the Eastern Fold Belt (EFB), and to better correlate these rocks with those in other parts of the Mount Isa Inlier and in other Proterozoic inliers of northern Australia (Page & Sun in press: Australian Journal of Earth Sciences; Page et al. 1997: Abstracts, Geodynamics and Ore Deposits Conference, Australian Geodynamics Cooperative Research Centre, Ballarat, Victoria, 46–48). The results have clear relevance to metallogenic exploration in the EFB.

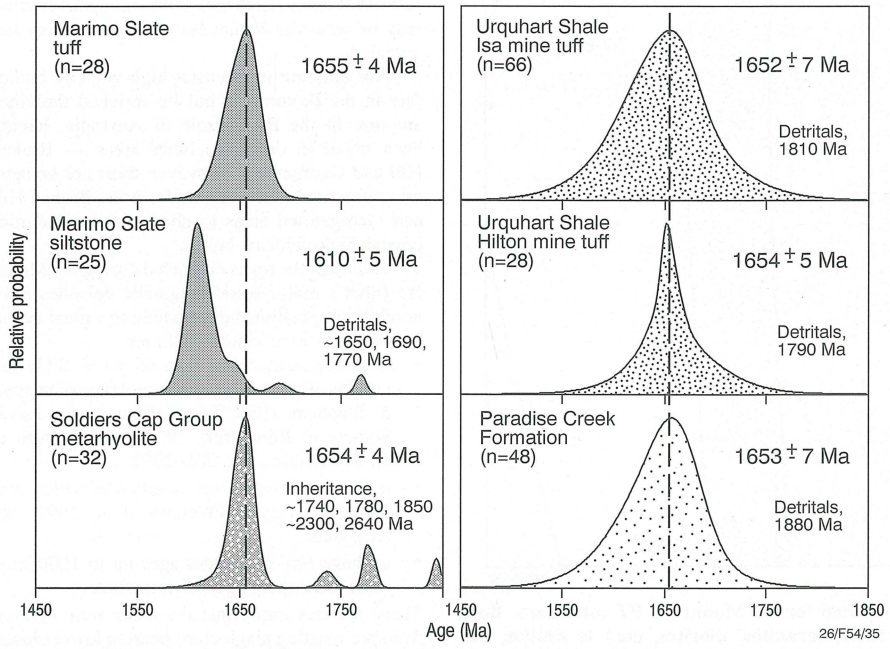

Fig. 17. Relative age probabilities in the SHRIMP U–Pb zircon data from the Marimo Slate and Soldiers Cap Group. Also illustrated are the relative age probabilities showing the similar ages for the Urquhart Shale (Mount Isa Group) and Paradise Creek Formation (McNamara Group) from Page & Sweet (in press). The dashed vertical line represents 1655 Ma.

Soldiers Cap Group

The EFB contains elements of both older (~1750 Ma) and younger (~1655–1680 Ma) tectonostratigraphic packages (cover sequences 2 and 3 in the terminology of Blake 1987: BMR [AGSO] Bulletin 225). An important outcome from the new EFB geochronology is that siliciclastic rocks and mafic volcanics of the Soldiers Cap Group (including the paragneiss that hosts the Cannington Ag–Pb–Zn deposit) are firmly placed in the younger package — and are possibly as young as the ~1655 Ma Mount Isa and McNamara Groups of the Western Fold Belt. Whether they reflect high or low metamor-

phic grade, the Soldiers Cap Group rocks generally yield similar maximum depositional ages. Some of these ages have been documented previously (Page 1993: AGSO Research Newsletter 19, 4–5).

A U–Pb zircon age of 1654 ± 4 Ma has been obtained on a metarhyolite within the Soldiers Cap Group. This suggests that some of the earlier documented Soldiers Cap Group maximum ages might also be depositional ages, and points to a possible chronostratigraphic link between the Soldiers Cap Group and Mount Isa Group. Within the Mount Isa Group, the Urquhart Shale has been dated at Mount Isa and Hilton at 1652 ± 7 Ma and 1654 ± 5 Ma respectively (Page & Sweet in press: Australian Journal of Earth Sciences).

Marimo Slate and Tommy Creek Block

With components between 1620 and 1650 Ma old, the rocks in the Tommy Creek Block have previously demonstrated their connection with a depositional regime as young as or younger than the Mount Isa Group (Page 1983: Precambrian Research, 21, 223–245; Hill et al. 1992: AGSO Bulletin 243, 329–348).

The Marimo Slate (southeast of the Tommy Creek Block) forms a synclinal structure bounded in the west by the Duck Creek Anticline, and is evident in the Mount Isa seismic reflection data as a possibly younger package. New SHRIMP geochronology on a felsic tuff and a tuffaceous siltstone from the Marimo Slate (hitherto part of the ~1750-Ma Mary Kathleen Group package) indicates depositional ages of 1655 ± 4 Ma and 1610 ± 5 Ma. These results further point to the importance and wider distribution of the younger cover rocks in the eastern part of the inlier. Although the stratigraphic relationship between the two dated, isoclinally folded rocks is not known, the clear difference in their ages indicates at least one time break in Marimo Slate deposition. This is emphasised by the possibility that the 1610 ± 5 Ma age might be a maximum age for deposition.

Like parts of the Soldiers Cap Group (and rocks in the Tommy Creek Block) the Marimo Slate now can be confidently linked in time with the Mount Isa and McNamara Groups in the west; this is evident from the age probability diagrams (Fig. 17).

Exploration significance of the new data

Large parts of the EFB stratigraphy have now been shown to be Mount Isa Group equivalents, which clearly enhances their base-metal prospectivity. The presence in the middle part of the Marimo Slate of carbonaceous shale and base-metal anomalies (Derrick et al. 1971: BMR Record 1971/56), and the proposal by Nye & Rayner (1940: Aerial, Geological & Geophysical Survey of Northern Australia, Queensland Report 35) that the Marimo Slate was part of their 'Mount Isa Series', could now refocus some exploration strategies.

[1] Minerals Division, Australian Geological Survey Organisation, GPO Box 378, Canberra, ACT 2601; tel. and fax +61 6 249 4261; e-mail rpage@agso.gov.au.
[2] Department of Earth Sciences, Monash University, Clayton, Victoria 3168; tel. +61 3 9905 4878; fax +61 9905 5062; e-mail tylermac@artemis.earth.monash.edu.au.
[3] Australian Geodynamics Cooperative Research Centre.

Recent tectonics and landscape evolution in the Broken Hill region

David L. Gibson

As part of the Broken Hill Exploration Initiative, recent landform and regolith investigations, and the interpretation of data acquired from recent AGSO seismic and aeromagnetic surveys, have distinguished several tectonically influenced landscapes in the Broken Hill region. These landscapes have resulted from deformation linked to post-Early Cretaceous reactivation of pre-existing faults. Their reactivation was due to a probable easterly to southeasterly oriented palaeostress field which influenced thrust-faulting along low-angle north-northwesterly to northeasterly trending fault segments, and possible wrench-faulting along some northwesterly trending steeper segments.

The lithology, attitude, and elevation of poorly exposed post-Palaeozoic sedimentary rocks are important to this study. In particular, deformed Lower Cretaceous rocks (dated by palynology; M. Macphail, ANU, personal communication 1996) are present around the northern tip of the Broken Hill Inlier near Fowlers Gap (Fig. 18); previously undated, these rocks had been considered to be Eocene (Neef et al. 1995: Australian Journal of Earth Sciences, 42, 557–570). Similar rocks forming a poorly exposed veneer over Precambrian rocks on the Kantappa Fault Block (see below) are here also considered to be Cretaceous. Previously unmapped post-Palaeozoic rocks in the Scopes Range and Dolo Hills have yet to be dated.

The Mundi Mundi and Kantappa Faults

The Mundi Mundi Fault (Fig. 18) defines a curvilinear north-northeasterly trending scarp separating the western margin of the Barrier Ranges from the alluvial Mundi Mundi Plain. The fault is concealed below alluvium for most of its length, and its attitude has only recently been revealed. New AGSO seismic reflection data show that it is a major crustal structure dipping about 30°E (K. Wake-Dyster, AGSO, personal communication 1996). Refraction data (A. Owen, AGSO, personal communication 1996) indicate that about 200 m of low-velocity material underlies the Mundi Mundi Plain and thickens eastwards towards the scarp (Fig. 19).

Shot-hole cuttings, and exposures in dissected fans near the scarp, show that at least the top 40 m of this material is reddish alluvium. Elsewhere on the plain, company drilling (B. Stevens, Geological Survey of New South Wales, & D. Lawie, University of New England, personal communication 1997) indicates that up to 100 m of alluvium with similar colour and composition overlies grey-green Lower to ?Upper Miocene lacustrine fine clastic and carbonate rocks (Namba Formation; Callan & Tedford 1976: Transactions of the Royal Society of South Australia, 100, 125–168), and possibly lower Tertiary and Lower Cretaceous rocks, which in turn unconformably overlie Precambrian rocks at depths of up to 200 m. Hence, the available evidence suggests that about half the low-velocity material is red alluvium, whose stratigraphic position, and dating at the surface (500 to >16 500 y; Wasson 1979: Sedimentary Geology, 22, 21–51), suggest a Pliocene to Holocene age.

The arrangement of landscape (including summit concordance in the Barrier Ranges) and sediments (Fig. 19) is consistent with the Barrier Ranges being a dissected zone at the margin of an upthrust tilt-block which had low local relief before uplift. Vertical displacement of about 400 m is suggested in the vicinity of the seismic line. The thickening of low-velocity material immediately west of the fault is here interpreted to represent downwarp from crustal loading associated with thrusting. Westerly flowing streams initiated by the uplift eroded the uplifted western margin of the tilt-block, and deposited the thick alluvium on the Mundi Mundi Plain. The age of this syntectonic alluvium, as discussed above, indicates that uplift mostly occurred in the Pliocene to Pleistocene. The exposed alluvium shows no evidence of faulting, suggesting that Holocene movement has not occurred.

A low scarp mapped as the Kantappa Fault (Fig. 18) branches northwesterly from the Mundi Mundi Fault scarp at about latitude 31°30′S. It separates rises of eroding alluvium and weathered bedrock capped by a discontinuous veneer of ?Cretaceous rocks to the northeast from alluvial and aeolian sand plains to the southwest. North of this point, the Mundi Mundi Fault scarp is less well

defined: the dissected area to the east has lower elevation and relief; large sediment-filled re-entrants punctuate the scarp line; locally extensive, sloping bedrock pediments immediately underlie the scarp; and aeromagnetic data suggest that the alluvium to the west of the scarp has no great thickness.

Magnetic data also show a sharp boundary between thick alluvium to the southwest and bedrock to the northeast. This boundary coincides with the Kantappa Fault scarp, and continues along the Mundi Mundi Fault scarp to the south. There is little or no magnetic indication of the Mundi Mundi Fault north of its junction with the Kantappa Fault. The magnetic data also show that the Kantappa Fault swings to the north, and coincides with the western margin of a series of low, lag-clad weathered bedrock rises with entrenched drainage.

The Kantappa Fault Block, bounded by the Mundi Mundi and Kantappa Faults, is interpreted as an east-tilted structural terrace (Fig. 20) whose near-surface rocks comprise mostly highly weathered bedrock capped by an eastward-thickening veneer of Cretaceous rocks and younger alluvium. Company drilling suggests that this veneer is up to 100 m thick in the east (B. Stevens, personal communication 1997). The foregoing data suggest that displacement during the early stages of thrust-faulting was mostly along the Mundi Mundi Fault, which subsequently 'locked', and movement was transferred to a westward splay, the Kantappa Fault.

Scopes Range and Dolo Hills

The Scopes Range (Fig. 18) is a fault-bounded, northeasterly trending range of deformed Palaeozoic sedimentary rocks. A previously undescribed flat-lying sequence of fluvial, poorly cemented pebbly sandstone and conglomerate up to 15 m thick is locally present near the crest of the range. Possibly

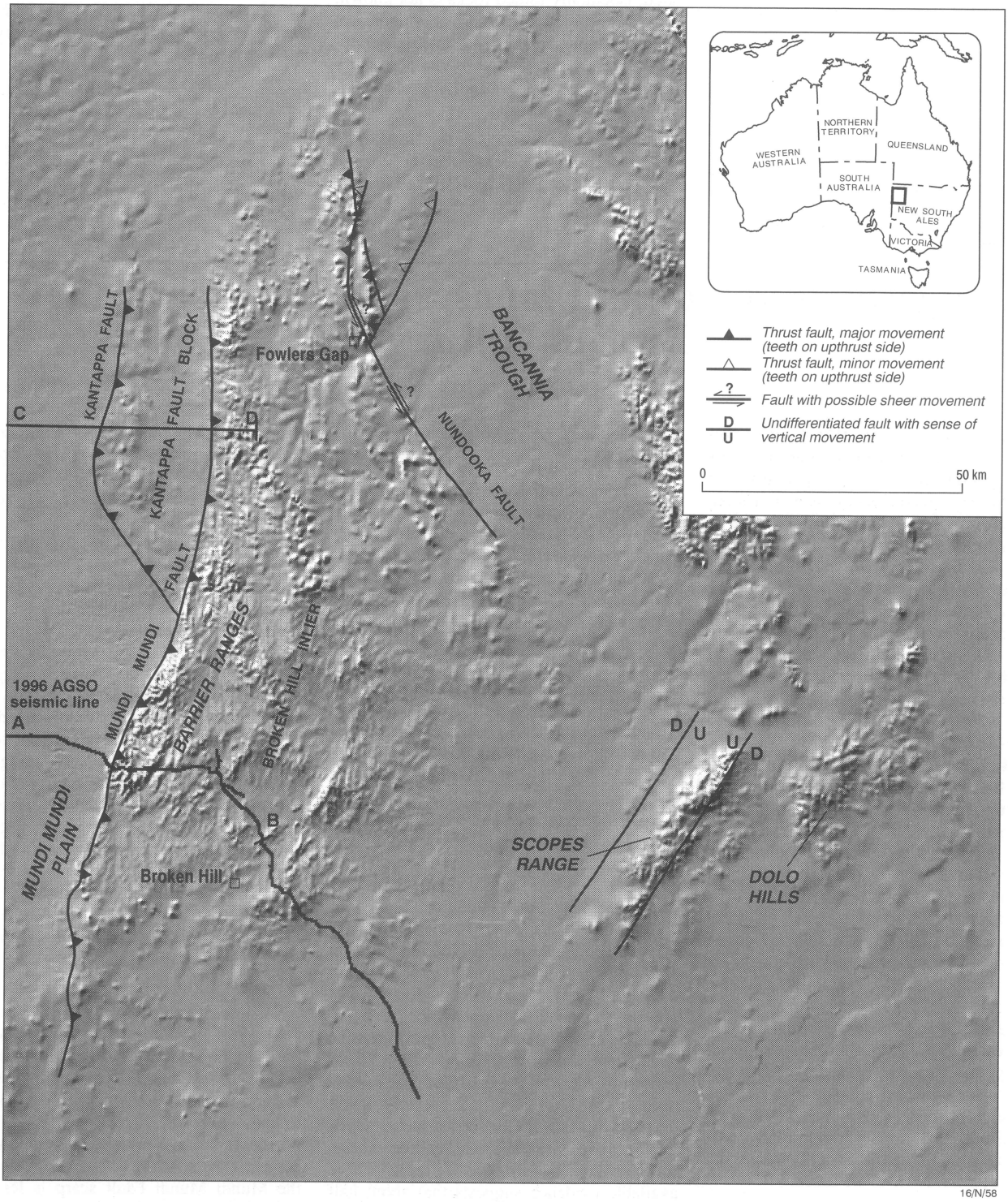

Fig. 18. Greyscale elevation model of the Broken Hill region showing interpreted faults with post-Early Cretaceous movement.

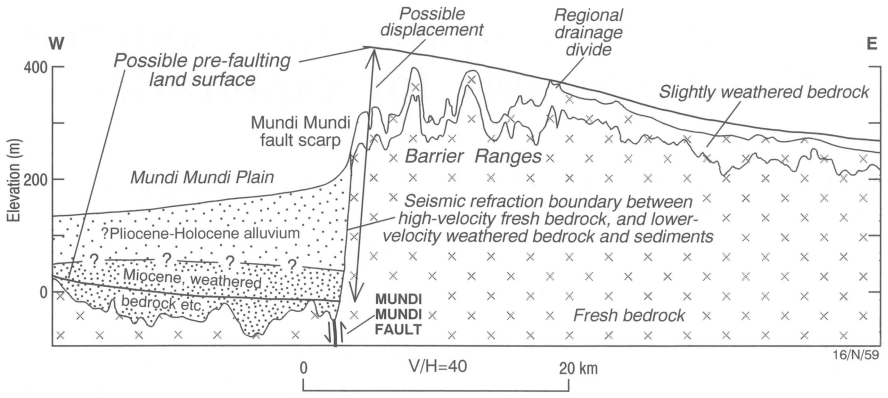

Fig. 19. Section across the Mundi Mundi Fault. A. Owen (AGSO) supplied the refraction and elevation data. Section A–B in Figure 18.

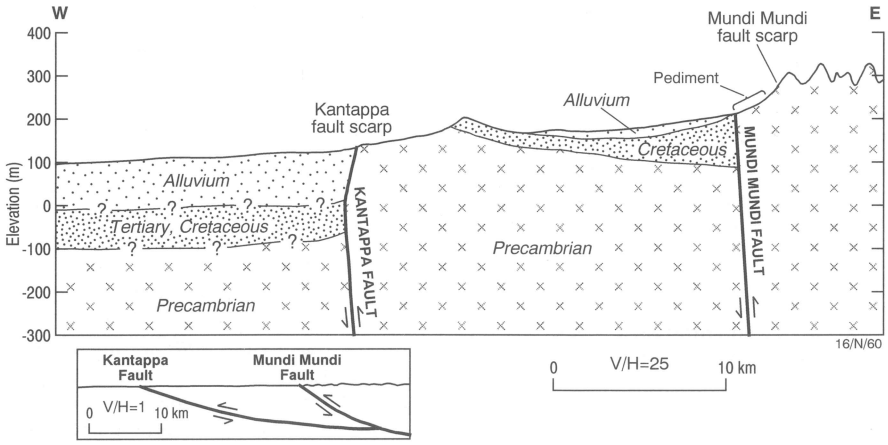

Fig. 20. Interpreted sections with exaggerated and uniform scales across the Kantappa Fault Block. Detailed topographic data were derived from AGSO airborne geophysical surveys. Section C–D in Figure 18.

equivalent rocks are exposed on the adjoining plain to the southeast. It is here interpreted that the range had little relief when the flat-lying sequence accumulated, and that relative uplift of at least 50 m has occurred since. The range most likely represents a horst, and a continuation of the northeasterly trending sub-Murray Basin Scopes Range High, identified from geophysics (e.g., the 1996 AGSO seismic and aeromagnetic surveys) about 40 km to the southwest.

Post-Palaeozoic sedimentary rocks have also been identified in the Dolo Hills (Fig. 18), at elevations differing by over 70 m. Again this suggests tectonic dislocations, but mechanisms of displacement have yet to be identified.

Fowlers Gap area

Devonian sandstone forming ranges north of Fowlers Gap (Fig. 18) is unconformably overlain by poorly exposed easterly dipping Lower Cretaceous sandstone, shale, and conglomerate at the western margin of the Bancannia Trough. The previously unmapped surface trace of the base-Cretaceous unconformity generally occurs at the break of slope at the eastern margin of the ranges. Small outliers of correlatives of the Cretaceous rocks are locally present on and to the west of the ranges. Analysis of the pattern of dips in the Devonian rocks, and the elevation and attitude of the Cretaceous rocks, indicate that the ranges result primarily from uplift associated with monoclinal flexing of uniformly easterly dipping Devonian rocks and unconformably overlying horizontal Cretaceous rocks (Fig. 21).

Post-deformational erosion, which has removed most of the poorly consolidated Cretaceous rocks to near local base level and etched the generally more resistant Devonian rocks, has shaped the present topography of the ranges. The deformation probably resulted from thrusting at depth on a westerly dipping fault system that includes the previously mapped Nundooka Fault, which also displaced the rocks during the Palaeozoic. The interpreted plan geometry of the fault system (Fig. 18) suggests that it may constitute a flower structure formed by the interaction of sinistral wrenching and a northward deflection in the north-northwest trend of the Nundooka Fault.

Synthesis

The pattern of post-Early Cretaceous fault displacement in the Broken Hill region is consistent with easterly to southeasterly shortening. Some low-angle faults oblique to this direction have been reactivated as thrust-faults, but the near-surface movement of some has been translated to monoclinal folding rather than displacement. Steeper faults oblique to the principal stress may have been reactivated as wrench faults. Movements have been sufficient to result in vertical displacement of up to 400 m.

The interpreted palaeostress direction contrasts with indications of a present-day easterly to northeasterly oriented principal stress computed from earthquake focal mechanisms and in situ stress measurements in the region (K. McCue, AGSO, personal communication 1997; Denham & Windsor 1991: Exploration Geophysics, 22, 101–105).

Latest Pliocene–earliest Pleistocene uplift of the MacDonnell Ranges has been reported by Senior et al. (1995: AGSO Journal of Australian Geology & Geophysics, 15, 421–444) in the Alice Springs region in central Australia, and linked to roughly north–south compression (R.D. Shaw, AGSO, personal communication 1997). Callan & Tedford (1976, op. cit.) inferred vigorous uplift of the Flinders Ranges (250 km west of Broken Hill) in the Late Miocene to Early Pliocene. Much of the tectonism described in this article probably occurred at a similar time, especially the movement along the Mundi Mundi–Kantappa Fault system. A time of higher stress in the general central Australian region during the late Cainozoic is suggested, but with stress directions different from those of today. The changing configuration of the northern margin of the Indo-Australian plate as it migrated northward and interacted with the Pacific, Philippine, and Eurasian Plates provides a mechanism for changes in stress direction and intensity during the Cainozoic.

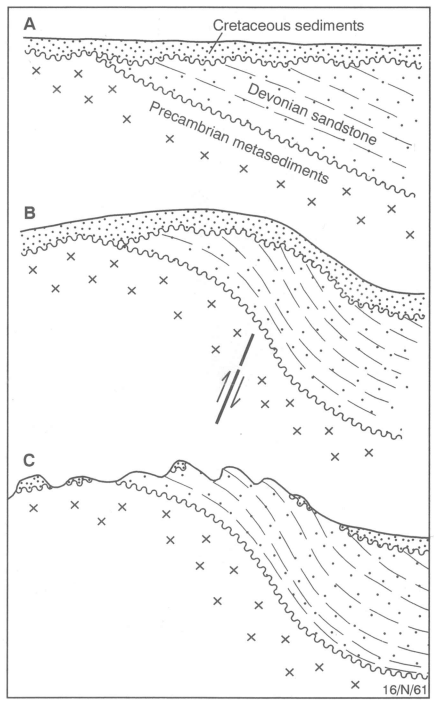

Fig. 21. Interpreted stages of development of the ranges north of Fowlers Gap by post-Early Cretaceous deformation and erosion. (A) Deposition of Lower Cretaceous sediments over uniformly dipping Devonian and deformed older rocks. (B) Monoclinal folding and uplift due to thrusting at depth. (C) Erosion of the uplifted areas imparts the present-day features of the ranges.

There is no indication that major fault movements in the Broken Hill region have continued into the Holocene, a feature that contrasts it with the Flinders Ranges, which continue to be tectonically active.

The distribution of the tectonically influenced landscapes, and the degree to which a possible weathered mantle and cover sequence has been stripped from uplifted areas, provide a useful framework for further regolith studies in the region.

Acknowledgment

My thanks go to George Gibson and Russell Shaw (AGSO) and Steve Hill (CRC LEME, ANU) for stimulating discussions on this subject.

[1] Cooperative Research Centre for Landscape Evolution and Mineral Exploration (CRC LEME); Minerals Division, Australian Geological Survey Organisation, GPO Box 378, Canberra, ACT 2601; tel +61 6 249 9748; fax +61 6 249 9983; e-mail dgibson@agso.gov.au.

Why sequence stratigraphy and not lithostratigraphy for exploration?

M.J. (Jim) Jackson[1], Rod Page[1], Peter Southgate[1], & Deb Scott[1]

Intriguing results from recent field research and SHRIMP zircon dating of rocks from the Palaeoproterozoic McArthur Basin, northern Australia, illustrate why a modern *sequence stratigraphic* approach to studying sedimentary successions is likely to provide better results than a more traditional *lithostratigraphic* approach. The sequence stratigraphic approach facilitates an improved understanding of stratal relationships by providing a chronostratigraphic framework for correlation and mapping. It also encourages the identification of subtle but possibly significant breaks in sedimentation. As the Proterozoic successions of northern Australia contain several world-class sediment-hosted base-metal deposits, a better understanding of regional stratigraphic relationships and accommodation history is crucial to improving our ability to predict the distribution and lateral variability of potential host rocks, and the distribution of surfaces that control stratal fluid flow.

The Wollogorang Formation — a viable unit for resource mapping?

Applying lithostratigraphic mapping practices in the McArthur Basin, Roberts et al. (1963: 'Calvert Hills, NT — 1:250 000 Geological Series, SE/53–8', BMR [AGSO], Canberra) defined a unit called the Wollogorang Formation. This unit comprises a succession of dolostone, shale, and sandstone sandwiched stratigraphically between igneous rocks in the upper part of the Tawallah Group. The definition was extended and refined by Jackson et al. 1987 (BMR Bulletin 220), who mapped the unit through the Calvert Hills–Bauhinia Downs area. Because it contains a number of distinctive rock types and sedimentary structures, the Wollogorang Formation was used as a key stratigraphic marker during the mapping of the southern half of the basin in the 1980s (Fig. 22).

Later, during mapping of the northern part of the basin (Katherine to Arnhem Land region), a sedimentary unit (McCaw Formation) near the top of the Tawallah Group (and its equivalents) with a similar shaly dolomitic facies was also identified as an important local marker. It has been tentatively correlated with the Wollogorang Formation (Rawlings et al. in press, 'Arnhem Bay–Gove — 1:250 000 Geological Series, SD/53–3 and 4', Northern Territory Geological Survey and AGSO).

In a basin context, therefore, the Wollogorang Formation and its lateral equivalents are important stratigraphic markers.

During the initial field season of the NABRE ('North Australian basins resource evaluation') project in June 1995, the type section of the Wollogorang Formation, near Redbank (Figs. 22 and 23), was re-examined and reassessed from a sequence stratigraphic perspective. This revisit suggested that a prominent mid-unit sequence boundary (a marked break in sedimentation, or unconformity) separates the clastic facies (VIa) from the underlying dolostones and shales. Further, the upper and lower parts of the formation should perhaps be considered as parts of different basin phases and not parts of one genetic stratigraphic unit.

To provide an independent test for this hypothesis, primary igneous zircon in thin tuffaceous beds from drillcore samples above and below this possible chronostratigraphic surface have been dated. Preliminary U–Pb SHRIMP results evince a significant break.

Lithostratigraphy v. sequence stratigraphy

According to the Australian Stratigraphic Code (Geological Society of Australia 1964), '... the fundamental procedure in lithostratigraphy is to observe, describe and correlate

Fig. 22. Distribution of the main outcrops of the Wollogorang Formation in the southern McArthur Basin, and locations of drillholes sampled for zircon dating.

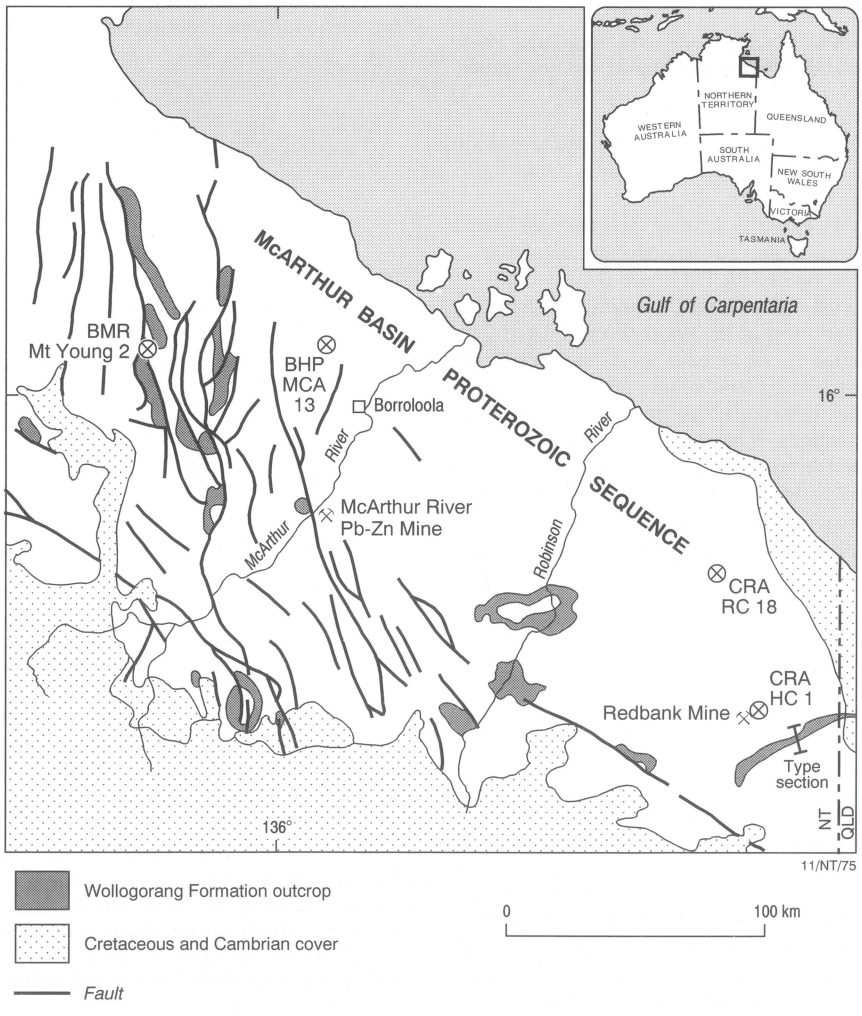

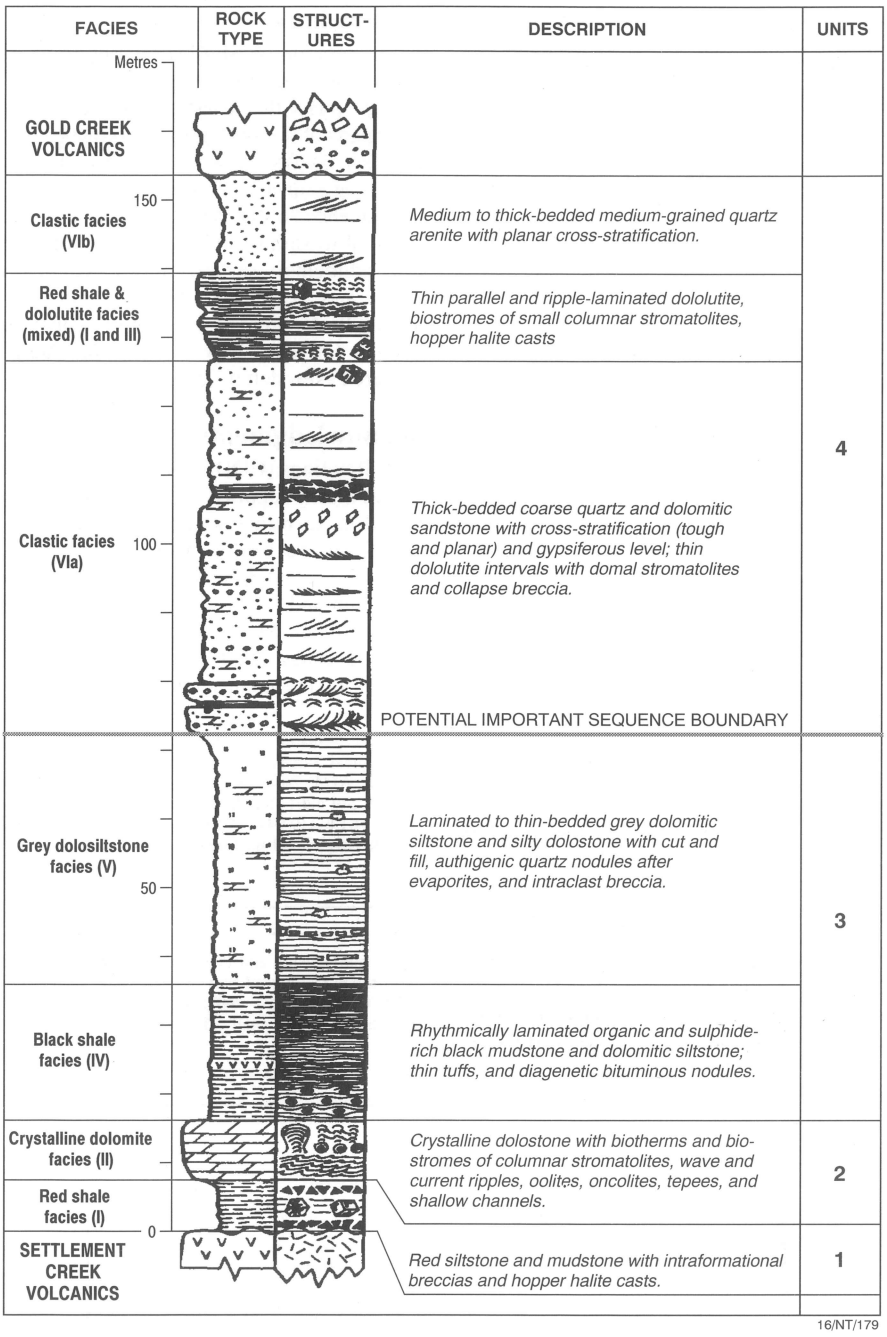

Fig. 23. Composite stratigraphic section of the Wollogorang Formation in the type area, near Redbank mine, as published in Jackson et al. (1987: op. cit., fig. 27).

sequences.'* Further, '... it is convenient to describe local successions in terms of named and defined units which should be described in terms of readily observable lithological characteristics (petrological, mineralogical, palaeontological, etc.).' In addition, 'The boundaries of each unit should be placed at *positions of lithological change*' and 'Boundaries are *not defined to imply isochronous surfaces*' (our italics).

Even though the Australian Code of 1964 has been superseded (Staines 1985: Australian Journal of Earth Sciences, 32, 83–106; Salvador 1994: 'International stratigraphic guide', 2nd edition, International Union of Geological Sciences and Geological Society of America), these principles remain the same. Hence, the basic process of lithostratigraphy is to identify, group, describe, and give names to mappable units.

This approach was applied to group together the sedimentary rocks — red shale, stromatolitic and oolitic dolostones, grey dolosiltstone, black shale with nodules, and dolomitic quartz sandstone — between the Settlement Creek Volcanics and Gold Creek Volcanics (Fig. 23), and define them as the Wollogorang Formation. The upper and lower contacts are sharp lithological changes from sedimentary to igneous rocks. The formation was then mapped throughout the basin, where it was seen essentially as a mixed but lithologically distinctive sedimentary unit bracketed by very different igneous units and associated coarse-grained clastics.

* In this sense, the term 'sequence' does not adhere to the strict definition applied to it in sequence stratigraphy.

In their monograph, Emery & Myers (1996: 'Sequence stratigraphy', Blackwell Science) provide the following simple definition for sequence stratigraphy: '... the subdivision of sedimentary basin fills into *genetic packages bounded by unconformities* and their correlative conformities.', and 'It is used to provide a *chronostratigraphic framework* for the correlation and mapping of sedimentary facies.' (our italics).

In our particular example, therefore, sequence stratigraphy would aim to break the Proterozoic succession into genetic associations of units that would have been laid down together in contiguous facies, and also to look for marked changes in the vertical stacking of facies that could represent significant breaks in sedimentation.

A sequence stratigraphic perspective of the Wollogorang Formation

In a sequence stratigraphic context, the sharp change in the middle of the Wollogorang Formation — from low-energy, laminated dolomitic siltstone and shale (deep depositional environments) to high-energy, trough cross-bedded coarse-grained clastic rocks (fluvial deposits) — would appear as a likely sequence boundary (at ~72 m, Fig. 23). Down-hole gamma-ray logs also indicate a sharp change in geophysical response at this level, corresponding to the marked facies change. These changes reflect a marked basinward shift in facies accompanied by probable subaerial exposure at this junction, which fulfils the key criteria for defining as a sequence boundary (Wilgus et al. 1988: 'Sea-level changes: an integrated approach', SEPM Special Publication 42).

According to sequence stratigraphic concepts, the rocks above and below this 'unconformity' were laid down as parts of very different genetic packages, and should therefore be treated separately. Hence, the potential for lithostratigraphy and sequence stratigraphy to see the same package of rocks from a very different viewpoint. Instead of laterally tracing a sedimentary unit constrained between two largely igneous units, the sequence stratigraphic approach would encourage tracing the sequence boundary laterally to assess its character and see how much of the underlying package has been removed. It would also emphasise looking laterally, but separately, for associations between the sedimentary facies and igneous facies above and below the sequence boundary.

A geochronological test of the sequence stratigraphic perspective of the Wollogorang Formation

Black shale in the lower Wollogorang Formation contains thin green mudstones interpreted as tuffaceous beds (Donnelly & Jackson 1988: Sedimentary Geology, 58, 145–169). Samples of the tuffaceous material were collected from Mount Young 2 and three other drillholes at widely spaced localities (Fig. 22). One of the drillholes, CRA HC1

contains tuffaceous material above and below the proposed sequence boundary.

The tuff layers in the black shale facies of the lower Wollogorang Formation are commonly around 20 cm thick. Their vitroclastic texture is evident from fine shard-like outlines now altered to a felted mass of fine white mica and chlorite. These features are consistent with the pristine igneous morphology of contained zircons, which should provide ages for the contemporary volcanism and, by implication, for the deposition of the enclosing black shale.

Two of the tuffs in Mount Young 2 are only a few metres apart stratigraphically. They have inseparable U–Pb SHRIMP zircon crystallisation ages of 1730 ± 3 Ma and 1729 ± 4 Ma. Fifty zircon analyses reveal no extraneous results, and, together with their isotopic concordance, suggest that these are stratigraphically meaningful ages.

A thicker tuff (36 cm) in the black shale facies of the lower Wollogorang Formation in CRA HC1 contains concordant, zoned igneous zircons and some older Palaeoproterozoic detrital grains. The main igneous population has an age of 1730 ± 3 Ma — identical with that of the shaly facies in Mount Young 2.

Some 62 m above this tuff in CRA HC1, a tuffaceous layer in the clastic facies of the upper part of the formation has been analysed in order to estimate the time break represented by the proposed sequence boundary. This tuff contains fewer zircons, of which several per cent are detrital grains up to 2000 Ma old. The igneous zircon population in this tuff is somewhat altered, possibly because of higher U content. Treatment of the most concordant U–Pb data gives an igneous crystallisation age of 1723 ± 4 Ma from 14 zircon analyses.

Despite the overlap in the 95% error limits, this result is statistically younger than the 1730-Ma results (at the 1% level using student's t test). We regard it as a useful stratigraphic age for the upper Wollogorang Formation. At face value, the results suggest a time break of several million years between the lower and upper parts of the Wollogorang Formation. The geological consistency of these results is being further evaluated by SHRIMP zircon analyses from other tuffs in the sequence near Wollogorang and Borroloola.

We note that the Hobblechain Rhyolite, about 200 m higher up in the Tawallah Group, has effectively the same age (1725 ± 2 Ma) as the upper Wollogorang tuff. This suggests that there is essentially no time break between the two, and that the intervening Gold Creek Volcanics were deposited quite rapidly. Alternatively, one or both of these ages is influenced by the presence of inherited zircons crystallised a few million years before the deposition of the tuff. These uncertainties are currently being addressed.

Conclusions

Preliminary zircon SHRIMP dating supports a significant age difference between the sedimentary rocks that constitute the lower and upper parts of the Wollogorang Formation, and has thus confirmed what was hypothesised mainly on sequence stratigraphic grounds.

Sequence stratigraphic concepts have the potential to significantly revise our ideas on how sedimentary successions are genetically linked, and, hence, how the mineral deposit-hosting Proterozoic basins in north Australia evolved (cf. Bradshaw et al. 1996: AGSO Research Newsletter 25, 21–22).

Acknowledgments

Dave Rawlings (CODES, University of Tasmania) kindly supplied unpublished data that helped us to refine some of the ideas presented here, but he does not necessarily agree with all the interpretations presented. We thank him and AGSO colleagues Ian Sweet, Albert Brakel, Mart Idnurm, Andrew Krassay, and Barry Bradshaw for their critical reviews of the manuscript.

[1] NABRE Research Team, Minerals Division, Australian Geological Survey Organisation, GPO Box 378, Canberra, ACT 2601; tel. +61 6 249 9205 (MJJ), +61 6 249 4261 (tel. & fax for RP), +61 6 249 9206 (PS), +61 6 249 9446 (DS), fax +61 6 249 9956 (MJJ, PS, & DS); e-mail jjackson@agso.gov.au.

Continued from facing page.

An attempt to correlate the loops and cusps with significant geological events in the Phanerozoic evolution of the North West Shelf is described in ***AGSO Record 1996/52***.

The review has highlighted an urgent need to improve Australia's Mesozoic polepath for better control in time and space on the plate-tectonic processes that shaped the main source and reservoir rocks of the North West Shelf.

[1] Minerals Division and Petroleum & Marine Division, Australian Geological Survey Organisation, GPO Box 378, Canberra, ACT 2601; tel. +61 6 249 9324, fax +61 6 249 9986, e-mail cklootwi@agso.gov.au.

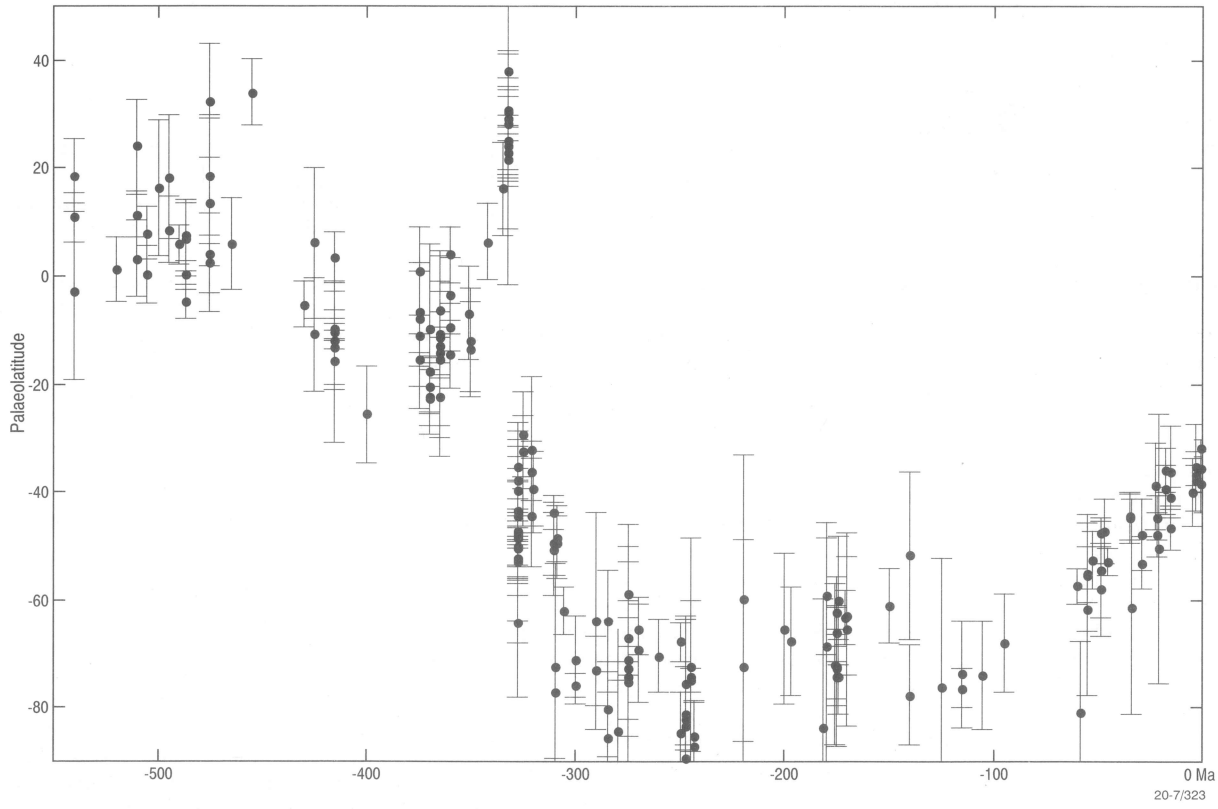

Fig. 24. Australian late Palaeozoic–Cenozoic polepath with approximate ages for loops and cusps shown.

Continued from back page.

The review demonstrated that several prevalent geodynamic models are depreciated by palaeomagnetic interpretations which are outdated owing to more recent palaeomagnetic developments or newly acquired geological information. Accordingly, Phanerozoic palaeomagnetic data of northeastern Gondwanaland have been re-examined for the main dispersive cratons (Australia and India), the main accretionary craton (Siberian Platform), and the continental fragments of established or presumed Gondwanan origin which became accreted onto Asia to the east of the Urals and onto the North American Cordillera.

Reconstructions

The re-examination of palaeomagnetic constraints focused particularly on the former location of the main Cathaysian landmass (the North China, South China, Indochina, and Tarim blocks) in northeastern Gondwanaland. Among other things, it revealed that the Cambrian to Late Devonian polepath trajectories for the North China block and Australia are superposed by rotation around an Eulerian pole that relocates North China off northwestern Australia and to the west of Irian Jaya (Fig.26A). This outcome is in good agreement with an independently derived reconstruction (Fig.26B) based on biostratigraphic and lithostratigraphic indicators (Metcalfe & Nicoll 1994: "Proceedings of the Symposium on 'Gondwana Dispersion and Asian Accretion'", IGCP Project 321). Previous attempts to relocate North China with respect to Australia were based on a comparison of individual pole positions of similar ages. Such a procedure leaves the palaeolongitudes indeterminate.

The unique lock on the relative Palaeozoic positions of North China and Australia provides a cornerstone for relocating other Cathaysian continents. Lacking more suitable data sets, such relocations have to be based on matching individual pole positions rather than on polepath fitting. The resulting palaeomagnetic reconstruction (Fig.26C), based on matching pole positions of about Middle Devonian age, is in good agreement with Metcalfe & Nicoll's reconstruction.

The re-examination also demonstrated some palaeomagnetic support for hypotheses that terranes now residing in the North American Cordillera (e.g., the Alexander terrane; Fig.26D) originated from the northeastern

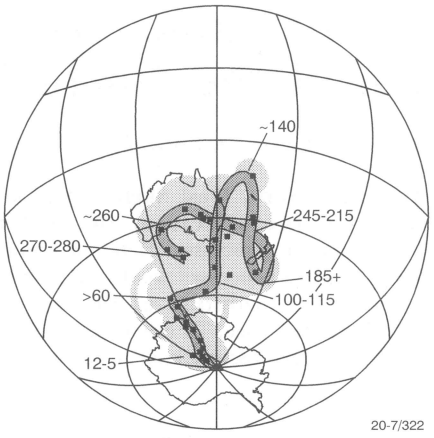

Fig. 25. Phanerozoic palaeolatitudinal evolution of Australia (Armidale reference location) according to data from cratonic Australia and the New England Orogen.

and eastern margins of Gondwanaland (e.g., Nur & Ben-Avraham 1983: in 'Accretion tectonics in the circum-Pacific regions', Terrapub, 3–18; Gehrels & Saleeby 1987: Tectonics, 6, 151–173).

Break-up phases

Dispersion of Greater Australia fragments that are now embedded in southern and eastern Asia has been mainly latitudinal, and obviously northward.

Fragments that now form part of the North American Cordillera and possibly also of northeastern Russia, however, probably dispersed initially eastward across the Panthalassa Ocean (palaeo-Pacific), before large-scale northward movement along the Cordillera and possibly beyond, along northern Siberia. These northward movement patterns show up clearly in plots of palaeolatitudinal evolution. An analysis of the palaeolatitude plots for separate fragments shows four northward movement phases of potential global relevance:

- Early Devonian (Kazakhstan);
- latest Devonian–middle Carboniferous (northeastern Gondwanaland);
- possibly middle to Late Permian (northeastern Gondwanaland); and
- Triassic (Cathaysian continents, northeastern Gondwanaland, Gondwanan fragments in southeast Asia, and terranes in the North American Cordillera).

These ages provide minima for the various phases of fragmentation of Gondwanaland's northeastern margin and, by implication, of the North West Shelf. The plots further identify southward rebound of northeastern Gondwanaland after each of the three later northward movement phases (Fig. 25). These three phases can be identified as geological events on the North West Shelf.

Loops and cusps on northeastern Gondwanaland polepaths

The Australian Phanerozoic polepath (Figs. 26A and 24; also cf. fig. 24 in Klootwijk 1995: AGSO Research Newsletter, 22, 14–17), supplemented by the Indian polepath, shows considerable potential to relate loops and cusps on the polepath to fundamental tectonic events that affected northeastern Gondwanaland, and subsequently the Australian and Indian plates after final breakup of Gondwanaland. Identified loops and cusps and available age constraints are:

Australia (age; Ma)	*India (age; Ma)*	*Loop/cusp*
€/O		loop
Dl (Ce)		cusp
Ce–l, 330–335		loop
Cl–Pe, 300		loop
Pe–l, 270–280 Ma		loop
~260		loop
~245–215	~250	cusp
~185+ Ma	210–200	loop
~140	130–150	loop
~100–115	<117>84	cusp
>60	~70	cusp
	~40–45	cusp
Tm–Tpl, >12<5		cusp

These loops and cusps on the polepaths probably reflect significant changes in global plate-movement patterns which might have resulted in tectonic phases, basin initiation, megashearing, etc. Far-field stresses originating from such changes can be transmitted widely across the lithosphere. Proper determination of the loops and cusps in space and time thus may provide important controls on, and — for periods before the oldest preserved (mid-Jurassic) seafloor-spreading patterns — the only effective means of:

- delineating changes in plate movements and resulting stress patterns; and
- predicting and dating the resulting tectonic events.

Continued on facing page.

Fig. 26A *(from back cover)*. **Reconstruction of the North China block's position with respect to Australia (and Gondwanaland) during the early Palaeozoic. The polepath trajectories and positions of these two Gondwanaland components were rotated 47.9° about an Euler pole at latitude 9.7°N and longitude 180.3°E. This Euler pole was derived from a visual superposition of splines fitted to a Cambrian to Late Devonian polepath trajectory for Australia and a Middle Cambrian to Late Devonian trajectory for North China. The North China block and fitted polepath are shown before and after rotation about the Euler pole. B. Reconstruction of northeastern Gondwanaland during the Late Silurian according to biostratigraphic and lithostratigraphic evidence (after Metcalfe & Nicoll 1994, fig.3). C. Middle Devonian palaeomagnetic reconstruction of the South China, Indochina, and Tarim blocks adjacent to the North China–Australia (Gondwanaland) composite (Fig.26A) according to a comparison of individual pole positions. This leaves the relative palaeolongitudes indeterminate. D. Early Devonian relocation of the North China–Australia (Gondwanaland) composite according to a 'splined' pole position for Australia (392.5 Ma). The shaded zone shows the palaeolatitudinal position and associated error for a reference locality on the Alexander terrane of the North American Cordillera. Note the agreement with the general palaeolatitude of the Lachlan Fold Belt.**

Geodynamic models and palaeomagnetic constraints on the evolution of the North West Shelf

Chris Klootwijk[1]

After the Middle Cambrian completion of the Rodinia-to-Gondwanaland transformation, northeastern Gondwanaland (i.e., 'Greater India' and 'Greater Australia') was fragmented, and the fragments were widely dispersed. An integral part of northeastern Gondwanaland, Australia's North West Shelf region has recorded the effects of the wider fragmentation processes. Detailed knowledge of these processes would help us to unravel the evolution of this major petroleum province. To this end, AGSO's Marine & Petroleum Division has undertaken a review of geodynamic models and palaeomagnetic constraints relevant to the Phanerozoic evolution of Gondwanaland's northeastern margin. The outcomes of this review have been documented as a set of *AGSO Records (1996/51, 52,* and *53*). The main findings are summarised below.

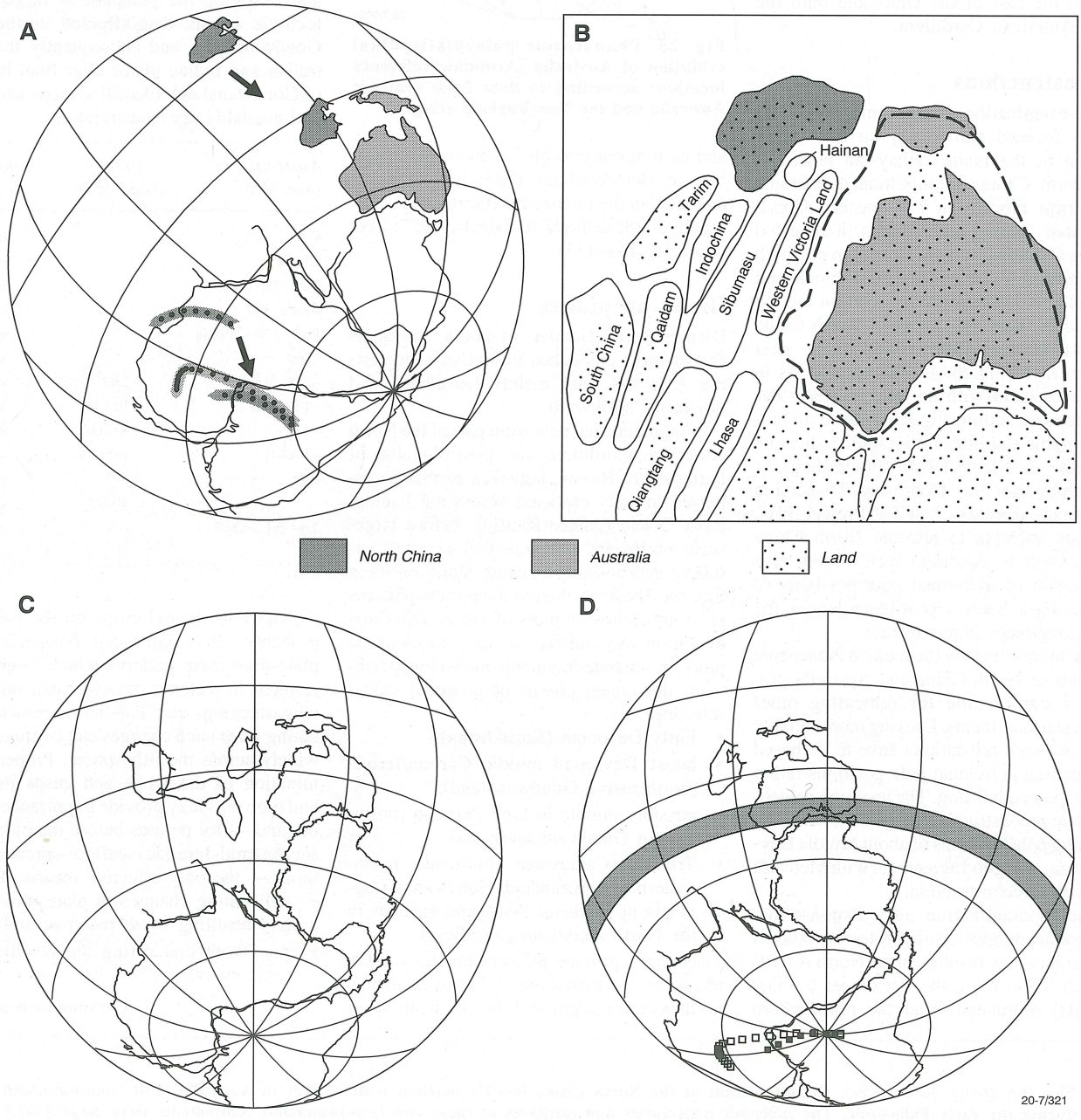

Caption on inside back cover (p. 23).

Continued on page 23.

The *AGSO Research Newsletter* is published twice a year, in May and November. The camera-ready copy for this issue was prepared by Lin Kay. Correspondence relating to the *AGSO Research Newsletter* should be addressed to Geoff Bladon, Editor, *AGSO Research Newsletter*, Australian Geological Survey Organisation, GPO Box 378, cnr Constitution Avenue & Anzac Parade, Parkes, Canberra, ACT 2601; tel. +61 6 249 9111, extn 9249; fax +61 6 249 9990, e-mail gbladon@agso.gov.au. An electronic version of this newsletter is accessible on the Internet at http://www.agso.gov.au/information/publications/resnews/
 ISSN 1039-091X PP255003/00266